NASA TECHNICAL NOTE

NASA TN D-5387

NASA TN D-5387

GASEOUS-HYDROGEN PRESSURANT REQUIREMENTS FOR THE DISCHARGE OF LIQUID HYDROGEN FROM A 3.96-METER- (13-FT-) DIAMETER SPHERICAL TANK

by Robert J. Stochl, Phillip A. Masters, Richard L. DeWitt, and Joseph E. Maloy

Lewis Research Center
Cleveland, Ohio

NATIONAL AERONAUTICS AND SPACE ADMINISTRATION • WASHINGTON, D. C. • AUGUST 1969

GASEOUS-HYDROGEN PRESSURANT REQUIREMENTS FOR THE DISCHARGE OF LIQUID HYDROGEN FROM A 3.96-METER-(13-FT-) DIAMETER SPHERICAL TANK

By Robert J. Stochl, Phillip A. Masters, Richard L. DeWitt, and Joseph E. Maloy

Lewis Research Center
Cleveland, Ohio

NATIONAL AERONAUTICS AND SPACE ADMINISTRATION

For sale by the Clearinghouse for Federal Scientific and Technical Information
Springfield, Virginia 22151 – CFSTI price $3.00

ABSTRACT

An experimental investigation was conducted to determine the effects of various physical parameters on the pressurant gas requirements during the pressurization and expulsion of liquid hydrogen from a 3.96-meter- (13-ft-) diameter spherical tank. The experimental results were also compared with results predicted by a previously developed analytical program. The experimental results show that injector geometry, inlet gas temperature, and tank pressure level have a strong influence on the actual pressurant gas requirements. There was fair agreement between the analysis and experimental data when using the hemisphere injector. However, the analysis in its present form does not adequately predict pressurant requirements when using the straight pipe injector.

GASEOUS-HYDROGEN PRESSURANT REQUIREMENTS FOR THE DISCHARGE OF LIQUID HYDROGEN FROM A 3.96-METER- (13-FT-) DIAMETER SPHERICAL TANK

by Robert J. Stochl, Phillip A. Masters, Richard L. DeWitt, and Joseph E. Maloy

Lewis Research Center

SUMMARY

An experimental investigation was conducted to determine the effects of various physical parameters on the pressurant gas (GH_2) requirements during the pressurization and expulsion of liquid hydrogen from a 3.96-meter- (13-ft-) diameter spherical tank. The experimental results were compared with results predicted by a previously developed analytical program which was revised and extended for this investigation. Tests were conducted for a range of outflow rates, pressurizing rates, and initial ullage volumes at nominal operating pressure levels of 24.13×10^4, 34.47×10^4, and 51.71×10^4 newtons per square meter (35, 50, and 75 psia) using inlet gas temperatures of 173 and 300 K (311° and 540° R). Data were obtained using two injector geometries, hemisphere and straight pipe.

The experimental results show that injector geometry, inlet gas temperature, and tank pressure level have a strong influence on the actual pressurant gas requirements. There was fair agreement between the analysis and experimental data when using a diffuser-type injector. However, the analysis in its present form does not adequately predict pressurant gas requirements when using the straight pipe injector.

INTRODUCTION

During the past several years, a great deal of effort has been devoted to the problems associated with the pressurized discharge of a cryogenic liquid from a tank. The main objective of these efforts has been the optimization of a propellant tank pressurization system. One phase of this optimization is a precise determination of pressurant requirements for any given set of operating parameters (i. e., tank pressure, inlet gas

temperature, liquid outflow rate, tank size, etc.). This knowledge would allow the design of a system that carried only the weight of gas necessary to accomplish the mission.

Several investigators have developed analyses (e.g., refs. 1 and 2) which attempt to predict, according to a selected set of simplifying assumptions, the quantity of pressurant gas required during the pressurized discharge of liquid hydrogen (LH_2). Some of these simplifying assumptions may, for certain conditions (i.e., for various injector geometries, tank shapes, and sizes), limit the capability of the analysis to accurately predict pressurant requirements.

Therefore, an investigation was conducted at the Lewis Research Center to determine experimentally the effects of various physical parameters on the pressurant gas requirements during the pressurization and expulsion of liquid hydrogen from propellant tanks. The experimental results were compared with results predicted by the analytical program developed in reference 1. Some results of this program are reported in references 3 and 4. The tests of reference 3 were performed in a 0.82-cubic-meter (29-ft^3) cylindrical (L/D = 3) tank using six different pressurant gas injection geometries. The pressurant gas used was hydrogen. The operating tank pressure level was 110.1×10^4 newtons per square meter (160 psi) with inlet pressurant gas temperatures between 282 and 310 K (508° and 558° R). The results of these tests showed that the analysis (ref. 1) for certain injector geometries could predict the actual pressurant requirements to within ±10 percent. The experimental results also indicated that between 10 and 20 percent of the total energy that was lost by the pressurant gas was lost to the liquid and that the mass transferred represented approximately 10 percent of the mass that was added to the tank through the injectors. Both mass and energy transfer between the pressurant gas and liquid are ignored by the analysis of reference 1.

The tests of reference 4 were performed in two 1.52-meter- (5-ft-) diameter spherical tanks (one had a wall thickness of 0.409 cm (0.161 in.), the other had one of 0.762 cm (0.30 in.)). Again, the pressurant gas used was hydrogen. The operating tank pressure level for these tests was 34.47×10^4 newtons per square meter (50 psia) with inlet gas temperatures of 167, 298, and 355 K (301°, 536°, and 639° R). The analysis of reference 1 was modified in reference 4 to incorporate the spherical tank geometry and also to incorporate an expression for the heat transfer from the gas to the liquid in the energy equation. The results showed that the modified analysis predicted the actual pressurant requirements for all conditions to within an average of 12.38 percent.

The analytical model and major assumptions used in references 3 and 4 thus proved to be adequate for relatively small cylindrical and spherical tanks. However, there was some doubt as to the validity of some of the assumptions for large scale tanks. This report presents the results of the investigation of the pressurant gas requirements in a 3.96-meter- (13-ft-) diameter spherical tank. The same modifications to the original analysis (ref. 1) that were used in reference 4 are used herein; that is, the analysis

was revised and extended to account for heat transfer occurring at the gas-liquid interface in tanks of arbitrary symmetric shape and was also extended to cover the initial pressurization period. For convenience, these modifications are presented in appendixes A, B, and C.

The major limiting assumptions remaining from the original analysis are those of one-dimensional flow and no mass transfer. References 3 and 4 both indicate that the assumption of one-dimensional flow is valid for injectors that diffuse the inlet pressurant throughout the ullage, but is not valid for straight pipe injectors. References 3 and 4 also indicate that mass transfer could, depending on the inlet gas temperature and the injector used, represent a substantial percentage of the pressurant requirement. However, the incorporation of mass transfer in the analysis was not attempted in this report because of the added complexity and incomplete knowledge of the mass transfer phenomenon.

The primary objective of the test work described herein was to obtain experimental values on the pressurant gas requirements during the pressurization and expulsion period in a 3.96-meter- (13-ft-) diameter tank for the various operation parameters and to compare these values with predicted ones. A secondary objective was to obtain experimental information on tank wall heating, liquid heating, residual ullage energy, and mass transfer in order to gain an insight into the reasons for (1) any variations in actual pressurant gas requirements, and (2) differences between predicted and experimental values.

The tests were conducted using a spherical aluminum tank located in a vacuum chamber. The main test variables were as follows:

Nominal inlet gas temperature, K (^{o}R)	173 and 300 (311 and 540)
Pressurant gas injector geometry	hemisphere and straight pipe
Nominal tank pressure, N/m^2 (psia)	24.13×10^4, 34.47×10^4, and 51.71×10^4 (35, 50, and 75)
Liquid outflow rates, kg/sec (lb/sec)	between 1.73 and 4.32 (3.81 and 9.52)

Data were also obtained for pressurization of the tank from 1 atmosphere to the desired operating pressure level at various rates from 2.59×10^3 to 10.14×10^3 newtons per square meter per second (0.376 to 1.47 psi/sec) for initial gas ullages of 5, 26, 52.5, and 74 percent of total tank volume.

SYMBOLS

A	area, m^2 (ft^2)
b	$1 - \frac{Z_1}{Z} - 2\frac{\Delta r}{r_i}$
C	orifice coefficient
C_H	effective perimeter of interior hardware, m (ft)
C_p	specific heat at constant pressure, J/(kg)(K) (Btu/(lb)(^oR))
C_v	specific heat at constant volume, J/(kg)(K) (Btu/(lb)(^oR))
C_w	specific heat of tank wall, J/(kg)(K) (Btu/(lb)(^oR))
c	$\alpha - \alpha\omega - T_w - \frac{1}{l_w \rho_w} \Delta t \frac{\dot{q}}{C_w}$
D	orifice diameter, m (ft)
d	$\frac{Z_2}{Z} \frac{\Delta X}{\Delta t} \frac{P' - P}{P'} - \frac{Z_1}{Z} \frac{\Delta X}{\Delta t}$
Gr	Grashof number, $\frac{L^3 \rho^2 g \beta \Delta T}{\mu^2}$
g	gravity acceleration, m/sec^2 (ft/sec^2)
H	enthalpy, J (Btu)
h	specèific enthalpy, J/kg (Btu/lb)
h_c	convective heat-transfer coefficient, $J/(m^2)(K)(sec)$ ($Btu/(ft^2)(^oR)(sec)$)
k	thermal conductivity, J/(m)(K)(sec) (Btu/(ft)(^oR)(sec))
L	flow length, m (ft)
l	thickness, m (ft)
M	mass, kg (lb)
ΔM	differential mass, kg (lb)
$\dot{M}$	mass flow rate, kg/sec (lb/sec)
$\overline{M}$	molecular weight, kg/(kg)(mole) (lb/(lb)(mole))
M_I	ideal pressurant requirement, kg (lb)
N	number of volume segments

Nu	Nusselt number, $\frac{h_c L}{k}$
n or i	summing index
P	pressure, N/m^2 $(lb/in.^2)$
ΔP	differential pressure, N/m^2 $(lb/in.^2)$
ΔP^*	orifice ΔP
Pr	Prandtl number, $\frac{\mu C_p}{k}$
Q	heat transfer, J (Btu)
$\dot{Q}$	heat-transfer rate, J/sec (Btu/sec)
$\dot{Q}'$	specific heat-transfer rate, J/(kg)(sec) (Btu/(lb)(sec))
$\dot{q}$	heat-transfer rate per unit area, $J/(m^2)(sec)$ $(Btu/(ft^2)(sec))$
R	gas constant, J/(K)(mole) $((ft\text{-}lb)/(^oR)(mole))$
r	radius, m (ft)
Δr	increment of radius, m (ft)
Re	Reynolds number, $\frac{L\bar{V}\rho}{\mu}$
T	temperature, K (^oR)
ΔT	differential temperature, K (^oR)
T_δ	temperature at edge of thermal boundary layer, K (^oR)
t	time, sec
Δt	time increment, sec
U	internal energy, J (Btu)
ΔU	differential energy, J (Btu)
u	specific internal energy, J/kg (Btu/lb)
V	volume, m^3 (ft^3)
ΔV	volume increment, m^3 (ft^3)
$\bar{V}$	velocity, m/sec (ft/sec)
v	specific volume, m^3/kg (ft^3/lb)
W	work, J (Btu)

Xn number of net points in ullage

x coordinate in direction of tank axis, m (ft)

Δx space increment, m (ft)

Y expansion factor

y thickness within boundary layer, m (ft)

Z compressibility factor

z elevation or vertical distance along tank wall, m (ft)

α $$\frac{1 + \dfrac{h_c \, \Delta t}{\rho_w l_w C_w}}{\left(\dfrac{2h_c RZ \, \Delta t}{r\bar{M}PC_p}\right)\left[1 + \left(\dfrac{\Delta r}{\Delta x}\right)^2\right]^{1/2}}$$

γ specific heat ratio

δ finite increment, or total boundary layer thickness, m (ft)

λ latent heat of vaporization, J/kg (Btu/lb)

μ viscosity, kg/(m)(hr) (lb/(ft)(hr))

ρ density, kg/m^3 (lb/ft^3)

ω $$\left(\frac{R}{\bar{J}\bar{M}} Z_1 \frac{\Delta P}{\Delta t} + \frac{RZ}{\bar{M}\pi r^2} \dot{q}\right) \frac{\Delta t}{C_p P}$$

β coefficient of thermal expansion 1/K ($1/^{o}R$)

Subscripts:

A analytical results

ad adiabatic

E experimental results

f final state or condition

G gas added to tank

H internal hardware

i initial state or condition

i → f from initial to final state or condition

L liquid

o condition prior to ramp

S liquid surface

sat saturation

T total quantity

t transferred

U ullage

w wall

Superscript:

' time index

APPARATUS AND INSTRUMENTATION

Facility

All tests were conducted inside a 7.61-meter- (25-ft-) diameter spherical vacuum chamber (fig. 1) to reduce the external heat transfer into the tank. The vacuum capa-

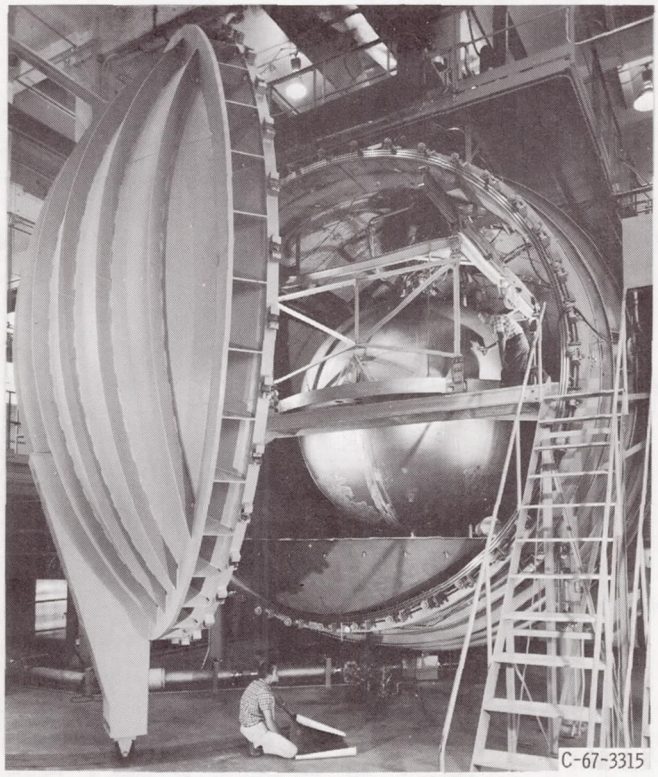

Figure 1. - 7.61-Meter- (25-foot-) diameter spherical vacuum chamber.

bility of this chamber was approximately 8×10^{-7} mm Hg. A general schematic of the test tank and associated equipment is shown in figure 2. The pressurant gas inlet temperature was controlled by a heat exchanger and blend valve subsystem capable of delivering gaseous hydrogen at temperatures between 167 and 405 K (301° and 729° R) at a maximum flow rate of 4.54×10^{-1} kilogram per second (1.00 lb/sec). A ramp generator and control valve were used for controlling the initial rate of pressurization of the propellant tank. A closed-loop pressure control circuit was used to maintain constant tank pressure during the expulsion period. The liquid outflow rate was controlled by remotely

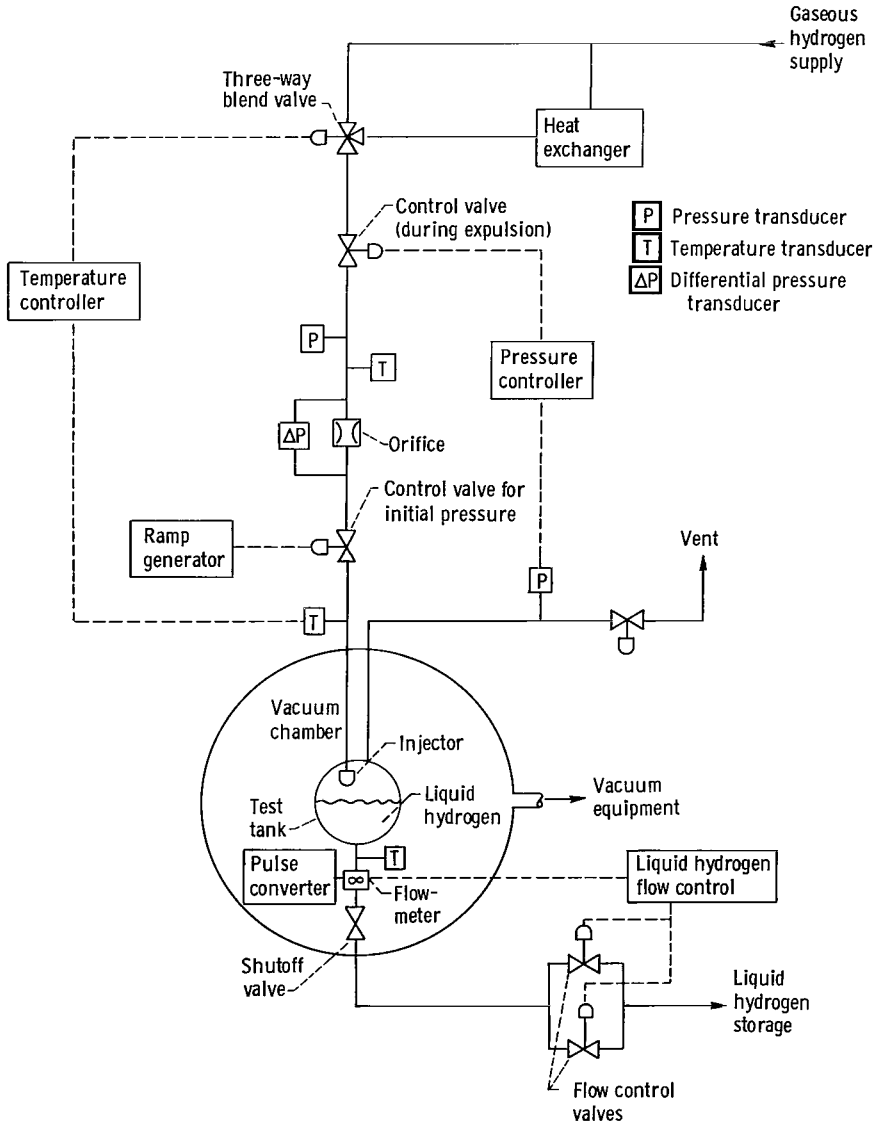

Figure 2. - General schematic of facility.

operated variable flow valves. The liquid hydrogen outflow from the tank was returned to the storage Dewar.

Liquid outflow rates were measured using a turbine-type flowmeter located in the transfer line. The flowmeter was calibrated, at the Lewis Research Center with LH_2, within an estimated uncertainty of ±1/2 percent over the expected range of flow rates. Pressurant gas inlet flow rates were determined by the use of an orifice located in the pressurant supply line. Tank, line, and differential pressures were measured with bonded strain-gage-type transducers to an estimated uncertainty of ±1/4 percent.

Test Tank

The experimental work was conducted in a 3.96-meter- (13-ft-) diameter spherical tank. The tank (fig. 3) was constructed of twelve 2219-T87 aluminum alloy gore segments. Each segment was chem-milled to three thicknesses. The weld land thickness was 1.95 centimeters (0.75 in.), the midland thickness was 1.27 centimeters (0.50 in.), and the membrane thickness was 0.89 centimeter (0.35 in.). The tank weight was 1800 kilograms (3769 lb). A 0.457-meter- (18-in.-) diameter flanged assembly was used as the lid of the tank. The lid, which housed the inlet and vent pipes and the electrical connections for all internal tank instrumentation, was constructed of 347 stainless steel and weighed 92.16 kilograms (203 lb).

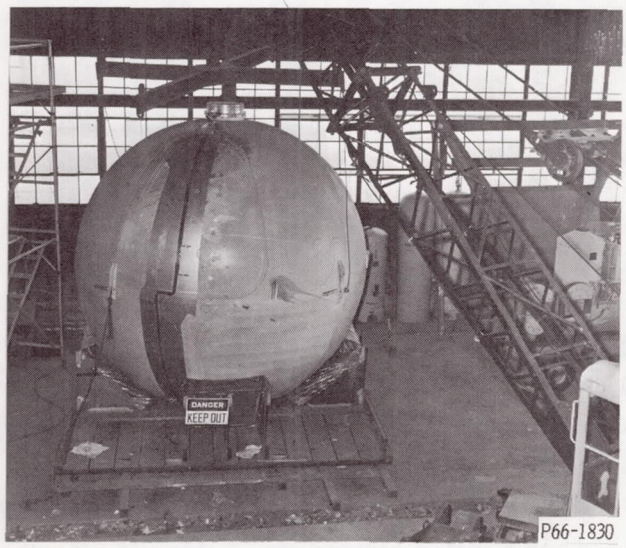

Figure 3. - 3.96-Meter- (13-foot-) diameter test tank.

Pressurant Gas Injector Geometries

The two injector geometries tested are shown in figure 4. These particular geometries were selected because they produce the two basic injection patterns of references 3 and 4. The hemisphere injector diffuses the pressurant uniformly throughout the ullage volume, while the straight pipe injects the pressurant gas in a concentrated jet toward the liquid surface. The hemisphere (which best seems to conform to the analytical assumption of one-dimensional gas flows) has an open exit area of 928 square centimeters (143.9 in.^{2}). The straight pipe injector had an open area of 17.15 square centimeters (2.66 in.^{2}).

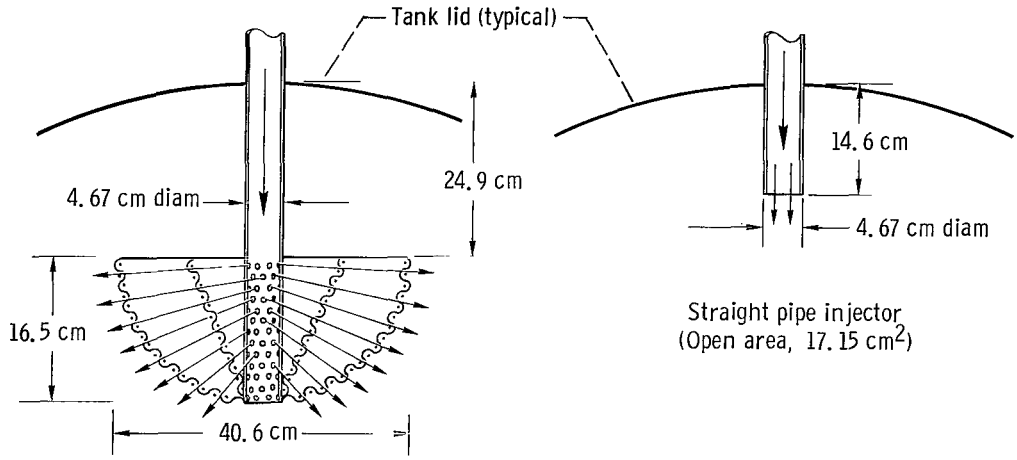

Figure 4. - Injector geometries.

Internal Tank Instrumentation

Ullage gas temperatures were used to determine the mass and energy content of the tank ullage. These temperatures were obtained with sensors capable of accurate measurement of rapid changes in temperature. Internal tank instrumentation is illustrated in figure 5. Location of the vertical and horizontal ullage gas temperature rakes are indicated. The thermopile was the basic temperature measurement technique used in this investigation. The use of thermopiles to measure ullage gas temperature was first described in reference 5, and the technique was used with good results in references 3 and 4. The main advantage of using thermopiles is their fast response time (between

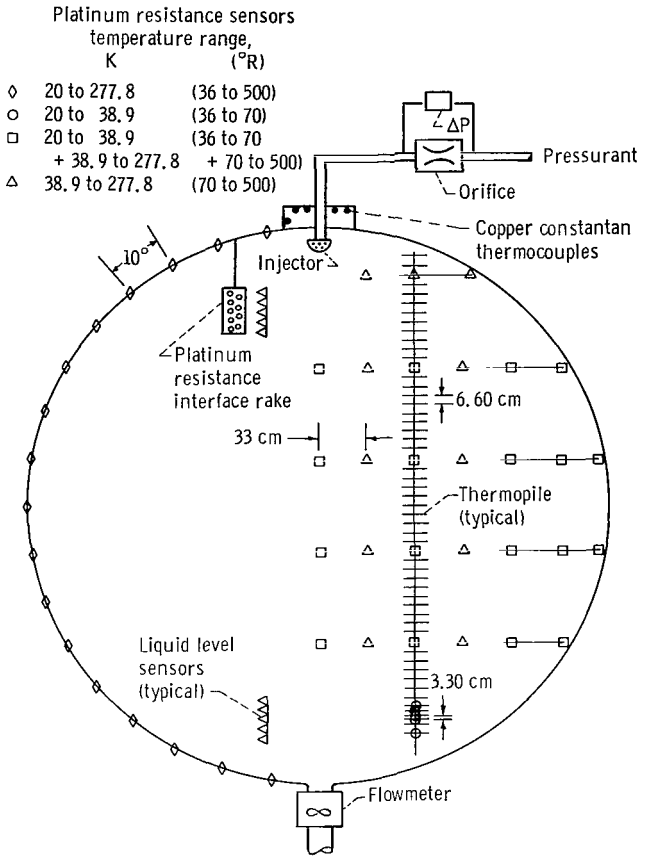

Figure 5. - 3.96-Meter-diameter tank instrumentation.

0.2 and 1.0 sec) in going from saturated liquid to saturated vapor. This time response is approximately an order of magnitude less than that of carbon resistors which also have been used in this type of investigation.

The instrumentation rake (fig. 6(a)) used in this investigation was an improved version of the rake used in reference 4. The sensors on this rake are more exposed to the surroundings than the sensors of reference 4. Triangular truss sections were used as the main support structure. The trusses were constructed of 0.476-centimeter- (0.187-in.) diameter stainless-steel tubing (fig. 6(a)) to minimize the heat capacity of the rake. Interlocking, laminated thermoplastic modules were used as the frame for the thermopile sensors.

A typical three-element thermopile unit wiring schematic is illustrated in figure 6(b). The thermopile units were constructed of 0.202 millimeter (0.008 in.) chromel-constantan wire. Vertical ullage gas temperature profiles were obtained by stacking the individual thermopile units as shown in figure 6(a). The spacing between the reference and measuring levels was 6.60 centimeters (2.60 in.) for the top 48 thermopiles of the

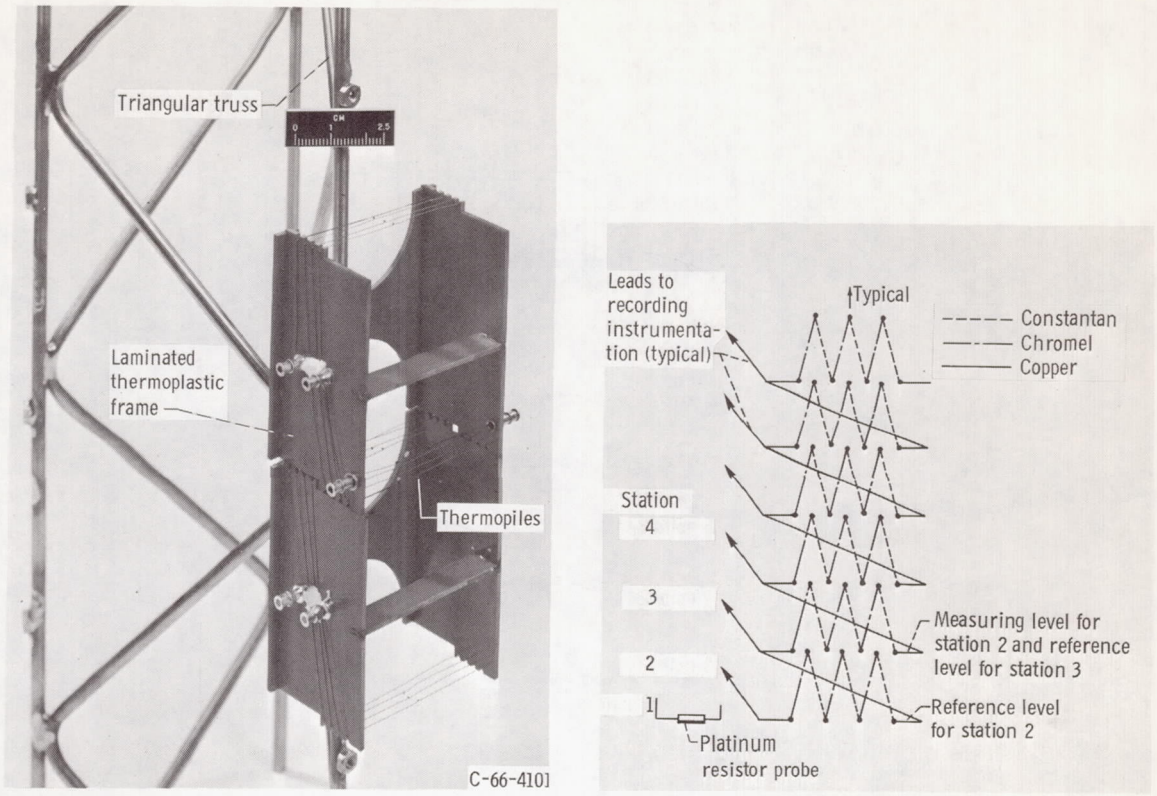

(a) Thermopile modules and support structure.

(b) Wiring schematic for rake.

Figure 6. - Thermopile rake.

vertical rake. The 8 units at the bottom of the rake had 3.30-centimeter (1.30-in.) spacings in order to obtain a more accurate temperature profile of the ullage gas near the liquid surface at the end of an expulsion.

Platinum resistance sensors, which were located at least every tenth station starting from the bottom of the rake, sensed the absolute temperature at their location and provided a reference for the thermopiles above the location. The horizontal rakes were composed of platinum resistance sensors spaced a maximum of 33.0 centimeters (13.0 in.) apart in the radial direction. Two platinum resistance sensors were used at each location to measure liquid and/or gas temperatures in the 20 to 38.9 K (36° to 70° R) and 38.9 to 277.8 K (70° to 500° R) ranges. These dual sensors permitted more accurate measurement of both liquid and gas temperatures than could be achieved with one sensor covering the entire range.

The initial static temperature profile near the liquid surface was determined by an interface rake (fig. 5). This rake contained 17 platinum resistance sensors spaced 1.10 centimeters (0.43 in.) apart. The range of these sensors was 20 to 38.9 K (36° to 70° R). The initial liquid level was determined by the location of the saturation temperature (corresponding to tank pressure) on the interface rake and verified by

liquid level sensors spaced 0.64 centimeter (0.25 in.) apart within the interface rake.

Platinum resistance sensors were also used to determine tank wall temperatures at 18 locations (every 10^{o} starting from the bottom of the tank) and the liquid temperature at the flowmeter. Copper-constantan thermocouples were used to determine tank lid temperatures at 5 locations and the pressurant gas inlet temperature.

All measurements were recorded on a high-speed digital data system. The measurements were recorded at a rate of 3.125×10^{3} channels per second. Each measurement channel was sampled every 0.064 second.

PROCEDURE

The spherical test tank was filled from the bottom to approximately a 2-percent ullage condition. It was then topped off as necessary while the tank lid and peripheral support hardware reached steady-state operating temperatures.

Temperature conditioning of the pressurant gas was then started. Gas flow was established through the heat exchanger loop, through the control valves and orifice arrangement, and then into the tank ullage from where it was vented through the conditioning line to the outside as shown in figure 2. The temperature control circuit shown in figure 2 was used to get the desired pressurant gas temperatures during the flow period. When the pressurant gas temperature conditioning was almost completed, the liquid level in the tank was adjusted to a desired value by either topping or slow draining. The liquid level was determined from the liquid level sensors on the interface rake.

The pressurant gas flow was then stopped and the test tank was vented in preparation for an expulsion run. The automatic controllers and timers were preset with all the desired run and operating conditions (i.e., tank pressure level, length of ramp period, length of hold period, liquid outflow valve position, start and stop times of the data recording equipment, etc.).

After starting the data recording equipment, the next step of the completely automatic run sequence was to take electrical calibrations on all pressure transducers. Immediately following this, the test tank was pressurized over a predetermined time base to the desired nominal operating pressure. Tank pressure was held constant for about 30 seconds to stabilize internal temperatures. The tank expulsion period was then started. The expulsion period was stopped when a hot wire liquid level sensor located at the 95-percent ullage level indicated gas. The test tank was then vented and refilled with LH_2 for the next expulsion.

Additional ramp pressurization runs, with no expulsion, were made for three different tank ullage levels. The only deviation in the operating procedure for these runs was that the liquid outflow valve was locked shut.

DATA REDUCTION

Physical Description of Problem

An initially vented tank containing a two-phase one-component cryogenic fluid was pressurized from 1 atmosphere to a higher pressure by adding gas to the ullage. The system was then allowed to reach a new equilibrium condition at which time liquid outflow was started. During the expulsion period, pressurant gas (at constant temperature) was added to the tank at a rate that maintained a constant tank pressure while expelling the liquid at a desired rate. The amount of pressurant gas used during the expulsion phase is dependent on (1) the volume of liquid displaced with no heat or mass transfer, (2) the heat transfer to the tank wall, internal hardware, and liquid, and (3) the amount of mass condensed or evaporated.

The main parameter used as a figure of merit in the subsequent discussion is the ratio of the ideal pressurant requirement to the actual pressurant requirement. The ideal pressurant was determined under the assumption that the incoming pressurant gas did not exchange energy or mass with the surroundings. Under this assumption, the ideal pressurant required for the initial pressurization of the tank was determined by the relation

$$M_I = \frac{\overline{M} P_o V_o}{Z R T_G} \left[\left(\frac{P_f}{P_o} \right)^{1/\gamma} - 1 \right] \tag{1}$$

The ideal pressurant required for the expulsion period was determined by the relation

$$M_I = \frac{\overline{M} P \, \Delta V_U}{Z R T_G} \tag{2}$$

Mass Balance

A mass balance was performed on the ullage volume from an initial time t_i to a final time t_f as follows:

$$M_{U,f} = M_{U,i} + M_{G,i \to f} \pm M_{t,i \to f} \tag{3}$$

A description is now given of the way in which the terms of equation (3) were determined.

Pressurant gas added ($M_{G,\,i\rightarrow f}$). - The weight of the actual pressurant gas used from any initial time t_i to any final time t_f was determined by numerical integration of the gas orifice equation:

$$M_{G,\,i\rightarrow f} = \int_{t_i}^{t_f} YD^2C\sqrt{\rho\,\Delta P^*}\,dt \tag{4}$$

Note that $t_f - t_i$ is the time necessary to expel ΔV_U of liquid.

Ullage mass. - The initial ullage mass $M_{U,\,i}$ and final ullage mass $M_{U,\,f}$ were obtained by numerical integration of the particular density profiles as follows:

$$M_{U,\,i} = \int_{V_{U,\,i}} \rho\,dV \simeq \sum_{n=1}^{N_i} \rho_n\,\Delta V_n \qquad \text{where } \rho = f(T, P) \tag{5}$$

$$M_{U,\,f} = \int_{V_{U,\,f}} \rho\,dV \simeq \sum_{n=1}^{N_f} \rho_n\,\Delta V_n \tag{6}$$

The internal tank volume was partitioned into 57 axial segments corresponding to thermopile location. Each of these segments was in turn divided into rings corresponding to the location of radial temperature sensors. These rings (339 in all) comprised the ΔV_n's in the previous calculations. In this manner, radial as well as axial temperature gradients could be incorporated into the mass calculations. The position of the liquid level prior to and after expulsion determined the number of gas volume rings (N_i and N_f) used in the ullage mass calculations.

Mass transfer. - The mass transfer was calculated from equation (3) as a result of knowing $M_{U,\,f}$, $M_{U,\,i}$, and $M_{G,\,i\rightarrow f}$; that is,

$$M_{t,\,i\rightarrow f} = M_{U,\,i} + M_{G,\,i\rightarrow f} - M_{U,\,f}$$

If $M_{t,\,i\rightarrow f}$ was a positive quantity, mass was assumed to be leaving the ullage volume (e.g., condensation).

Energy Balance

For the thermodynamic system consisting of the entire tank and its contents (tank + ullage gas + liquid), the first law of thermodynamics for an increment of time dt may be written, ignoring the potential and kinetic energy terms, as

$$dU_T = (\delta M_G)(u_G + P_G v_G) - (\delta M_L)(u_L + P_L V_L) + \delta Q - \delta W \tag{7}$$

If $h = u + Pv$ is substituted, equation (7) becomes

$$dU_T = (\delta M_G)h_G - (\delta M_L)h_L + \delta Q - \delta W \tag{8}$$

There is no external work done on the system so the final form of equation (7) becomes

$$dU_T = (\delta M_G)h_G - (\delta M_L)h_L + \delta Q \tag{9}$$

Equation (9) can be integrated over any time period. The physical interpretation of the quantities in equation (9) are as follows:

$$\underbrace{\int_{U_{t_i}}^{U_{t_f}} dU_T}_{\text{Change in system energy (tank+gas +liquid)}} = \underbrace{\int_{t_i}^{t_f} \dot{M}_G h_G \, dt}_{\text{Energy input by pressurant gas inflow}} - \underbrace{\int_{t_i}^{t_f} \dot{M}_L h_L \, dt}_{\text{Energy leaving through liquid outflow}} + \underbrace{\int_{t_i}^{t_f} \dot{Q} \, dt}_{\text{Energy from environment (heat leak)}} \tag{10}$$

A description is now given of the way in which the terms of equation (10) were evaluated.

Energy input by pressurant gas. - The first term on the right side of equation (10) can be evaluated as follows:

$$\int_{t_i}^{t_f} \dot{M}_G h_G \, dt \simeq \sum_{n=0}^{n = \frac{t_f - t_i}{\Delta t}} \dot{M}_{G,n} h_{G,n} \, \Delta t$$

The pressurant flow rate $\dot{M}_G$ was determined from equation (4). The specific enthalpy of the inlet gas was evaluated at the inlet temperature and pressure at each time increment Δt.

Energy leaving through liquid. - The energy of the liquid that leaves the system can be evaluated as follows:

$$\int_{t_i}^{t_f} \dot{M}_L h_L \, dt \simeq \sum_{n=0}^{n=\frac{t_f - t_i}{\Delta t}} \dot{M}_{L,n} h_{L,n} \, \Delta t \tag{11}$$

The liquid flow rate $\dot{M}_L$ was determined from the turbine flowmeter. The specific enthalpy of the liquid was evaluated at the outlet temperature.

Energy input from environment. - The rate of energy input into the tank from the environment was assumed to be the same for all tests and was determined from a boiloff test. This test resulted in a nominal value of energy input rate of 4.87×10^3 joules per second (4.66 Btu/sec). The total energy input over the expulsion period is given by equation (12). This value was, in all test cases, less than 8.2 percent of the energy added to the tank by the pressurant gas:

$$\int_{t_i}^{t_f} \dot{Q} \, dt \simeq 4.87 \times 10^3 (t_f - t_i) \tag{12}$$

Change in system energy. - The change in system energy can be separated into three categories: (1) change in ullage energy, (2) change in liquid energy, (3) change in the wall energy; or, stated mathematically,

$$dU_T = dU_U + dU_L + dU_w \tag{13}$$

Change in ullage energy. - The change in the ullage energy over any given time interval $t_i \rightarrow t_f$ is obtained by subtracting the internal energy of the ullage at time t_i from the internal energy at time t_f:

$$\int_{U_{t_i}}^{U_{t_f}} dU_U = \left(U_U\right)_{t_f} - \left(U_U\right)_{t_i} \tag{14}$$

Making use of the relation $U = H - PV$ gives

$$\int_{U_{t_i}}^{U_{t_f}} dU_U = \sum_{V_f} \rho_U \left(h_U - \frac{P}{\rho_U} \right) \Delta V_U - \sum_{V_i} \rho_U \left(h_U - \frac{P}{\rho_U} \right) \Delta V_U \tag{15}$$

The ullage gas density and enthalpy are functions of pressure and temperature. Therefore, the change in ullage energy was evaluated by knowing the pressure and temperature profiles at times t_f and t_i.

Change in liquid energy. - The change in energy of the liquid in the tank can be determined in a similar manner to the change in ullage energy:

$$\int_{U_{t_i}}^{U_{t_f}} dU_L = \left(U_L \right)_{t_f} - \left(U_L \right)_{t_i} \tag{16}$$

or

$$\int_{U_{t_i}}^{U_{t_f}} dU_L = \sum_{V_f} \rho_L \left(h_L - \frac{P}{\rho_L} \right) \Delta V_L - \sum_{V_i} \rho_L \left(h_L - \frac{P}{\rho_L} \right) \Delta V_L \tag{17}$$

Here again the liquid density and enthalpy are functions of measured pressure and temperature.

Change in wall energy. - The change in wall energy was determined by applying the first law of thermodynamics to an element of the wall:

$$\int_{U_{t_i}}^{U_{t_f}} dU_W = \Delta U_W = \Delta M_W \int_{T_1}^{T_2} C_v \, dT \qquad \text{where} \quad C_v = C_v(T) \tag{18}$$

The total change of the wall energy is then

$$\Delta U_{w,T} \cong \sum_{M_w} \left(\Delta U_w\right)_n \cong \sum \Delta M_w \int_{T_1}^{T_2} C_v(T)dT \tag{19}$$

Total energy distribution. - For convenience equation (13) is substituted into (10):

$$\int_{t_i}^{t_f} \frac{d}{dt}\left(U_U + U_w + U_L\right)dt = \int_{t_i}^{t_f} \dot{M}_G h_G \, dt - \int_{t_i}^{t_f} \dot{M}_L h_L \, dt + \int_{t_i}^{t_f} \dot{Q} \, dt \tag{20}$$

Rearranging terms gives

$$\underbrace{\int_{t_i}^{t_f} \left(\dot{M}_G h_G + \dot{Q}\right)dt}_{\substack{\text{Total energy} \\ \text{added } (\Delta U_T)}} = \underbrace{\int_{t_i}^{t_f} \left(\dot{M}_L h_L \, dt + dU_L\right)}_{\substack{\text{Total change} \\ \text{in liquid} \\ \text{energy} \\ (\Delta U_L)}} + \underbrace{\int_{t_i}^{t_f} dU_U}_{\substack{\text{Total} \\ \text{change} \\ \text{in ullage} \\ \text{energy} \\ (\Delta U_U)}} + \underbrace{\int_{t_i}^{t_f} dU_w}_{\substack{\text{Total} \\ \text{change} \\ \text{in wall} \\ \text{energy} \\ (\Delta U_w)}} \tag{21}$$

Dividing through by ΔU_T gives

$$1 = \frac{\Delta U_L}{\Delta U_T} + \frac{\Delta U_U}{\Delta U_T} + \frac{\Delta U_w}{\Delta U_T} \tag{22}$$

The data presented herein are in the form of these ratios which show the relative distribution of the total energy input.

Error Analysis

An analysis was performed to determine the magnitude of probable error which could be present in the integrations of equations (4) to (6) and in the determination of all terms in the energy balance equation (13). Probable error is defined as follows: There

TABLE I. - EXPERIMENTAL AND ANALYTICAL MASS BALANCE RESULTS

Run	Injector	Tank pressure, N/m^2	Volume discharge, m^3	Inlet gas temperature		Ramp time, sec	Hold time, sec	Expulsion time, sec	Tank cycle time, sec	Ramp			Hold				Expulsion				
				K	°R					Initial ullage mass, kg	Mass added during ramp, kg	Mass transfer during ramp, kg	Ullage mass after ramp, kg	Mass added during hold, kg	Mass transfer during hold, kg	Ullage mass after hold, kg	Mass added during expulsion, kg		Mass transfer during expulsion, kg	Final ullage mass, kg
																	Experimental	Analytical		
18	Hemisphere	34.47×10^4	28.40	300	540	18.30	34.76	1060.2	1113.26	1.168	0.248	-0.135	1.552	0.259	0.234	1.577±0.033	22.90±0.100	25.422	0.674±0.274	23.786±0.270
19	↓	↓	28.38	298	536	17.41	35.33	740.2	792.94	1.400	.215	-.098	1.713	.218	.289	1.642±0.105	21.02±0.070	22.395	1.121±0.259	21.524±0.237
20			28.38	298	536	16.77	35.77	457.2	509.74	1.756	.205	-.165	2.126	.214	.303	2.037±0.130	18.80±0.010	20.151	1.560±0.236	19.257±0.197
25			28.40	173	311	19.65	33.47	1062.9	1116.02	1.182	.422	-.106	1.711	.318	.288	1.740±0.088	27.19±0.014	32.269	.958±0.331	27.946±0.319
26			28.38	172	310	19.65	33.34	795.0	847.99	1.139	.436	-.088	1.662	.317	.174	1.805±0.117	26.24±0.010	30.435	1.043±0.322	26.983±0.300
27			28.38	170	306	19.58	33.28	468.9	521.76	1.221	.429	-.074	1.724	.330	.186	1.868±0.115	24.88±0.068	27.466	1.476±0.282	25.037±0.257
30	Straight pipe	34.47×10^4	28.38	292	526	38.08	64.13	1052.0	1154.21	1.365	0.284	-0.394	2.043	0.212	-0.057	2.312±0.079	15.47±0.072	27.534	-3.827±0.248	21.599±0.225
31	Straight pipe	34.47×10^4	28.38	292	526	37.44	64.38	780.0	881.82	.904	.288	-.613	1.806	.179	-.151	2.135±0.081	13.63±0.054	24.900	-5.531±0.241	21.288±0.227
34	Hemisphere	51.71×10^4	28.32	290	522	20.74	33.02	1158.1	1211.86	1.199	0.542	-0.034	1.775	0.427	0.253	1.948±0.023	31.39±0.012	35.600	1.760±0.331	31.552±0.330
35	↓	↓	↓	↓	↓	20.93	32.77	836.6	890.30	.864	.549	-.216	1.629	.440	.286	1.784±0.033	34.18±0.007	32.732	6.486±0.310	29.448±0.303
37						20.48	32.90	494.9	548.28	1.059	.526	-.147	1.732	.637	.542	1.827±0.039	30.09±0.008	28.911	5.080±0.263	26.611±0.260
39		24.13×10^4		285	513	19.01	34.56	1144.5	1198.07	1.031	.180	-.141	1.352	.206	.127	1.431±0.026	17.19±0.008	20.583	.213±0.226	19.114±0.224
40		↓		286	515	19.01	34.94	832.6	886.55	.891	.171	-.122	1.183	.178	.078	1.284±0.282	16.62±0.007	18.533	.499±0.346	17.392±0.191
42	↓	↓	↓	286	515	18.18	35.45	492.3	545.93	1.512	.154	-.107	1.773	.183	.193	1.763±0.257	14.71±0.007	15.790	1.132±0.304	15.328±0.161

TABLE II. - EXPERIMENTAL AND ANALYTICAL ENERGY BALANCE RESULTS

Run	Injector	Inlet gas temperature		Expulsion time, sec	Expulsion							
					Energy added by pressurant gas, J		Energy added by environment, J	Energy gained by tank wall, ΔU_W, J		Energy gained by ullage, ΔU_U, J		Energy gained by liquid, ΔU_L, J	
		K	°R		Experimental	Analytical		Experimental	Analytical	Experimental	Analytical	Experimental	Analytical
18	Hemisphere	300	540	1060.2	$96.35 \pm 0.04 \times 10^6$	98.24×10^6	5.213×10^6	58.78×10^6	52.23×10^6	$28.06 \pm 0.18 \times 10^6$	29.96×10^6	$17.27 \pm 1.87 \times 10^6$	16.05×10^6
19	↓	298	536	740.2	88.05 ± 0.03	81.65	3.639	52.90	44.00	27.06 ± 0.15	28.01	14.12 ± 1.65	9.64
20		298	536	457.2	78.41 ± 0.03	69.01	2.248	43.70	35.96	25.76 ± 0.11	27.13	7.94 ± 1.35	5.92
25		173	311	1062.9	66.35 ± 0.03	67.78	5.206	29.40	21.76	29.19 ± 0.21	32.17	16.95 ± 1.90	13.85
26		172	310	795.0	63.46 ± 0.03	62.31	3.909	26.94	20.64	28.71 ± 0.19	31.38	15.16 ± 1.69	10.29
27	↓	170	306	468.9	59.28 ± 0.02	54.02	2.305	22.10	17.84	27.61 ± 0.15	30.10	8.18 ± 1.38	6.08
30	Straight pipe	292	526	1052.0	$63.14 \pm 0.03 \times 10^6$	105.80×10^6	5.172×10^6	34.24×10^6	52.04×10^6	$26.13 \pm 0.12 \times 10^6$	30.80×10^6	$24.33 \pm 1.86 \times 10^6$	22.96×10^6
31	Straight pipe	292	526	780.0	55.72 ± 0.02	93.41	3.839	25.87	46.72	25.80 ± 0.11	29.64	25.23 ± 1.65	17.05
34	Hemisphere	290	522	1158.1	$126.72 \pm 0.02 \times 10^6$	127.59×10^6	5.694×10^6	70.56×10^6	62.23×10^6	$40.52 \pm 0.19 \times 10^6$	43.62×10^6	$21.65 \pm 1.96 \times 10^6$	21.75×10^6
35	↓	↓	↓	836.6	138.08 ± 0.03	114.64	4.113	67.45	56.60	39.51 ± 0.18	42.05	28.18 ± 1.72	16.00
37				494.9	121.21 ± 0.03	95.87	2.433	56.04	46.49	38.35 ± 0.14	39.96	13.27 ± 1.40	9.42
39		285	513	1144.5	71.75 ± 0.03	78.62	5.626	48.83	43.99	20.42 ± 0.17	21.89	14.59 ± 1.95	12.74
40		286	515	832.6	66.65 ± 0.03	67.38	4.093	43.86	37.22	19.72 ± 0.14	20.88	10.47 ± 1.71	9.27
42	↓	286	515	492.3	58.87 ± 0.03	56.38	2.420	36.35	31.19	18.49 ± 0.10	19.71	5.96 ± 1.42	5.49

is a 50-percent probability that the error will be no larger than the value stated. This analysis considered the errors introduced by the temperature transducers as well as the tank pressure sensor. The error analysis was performed for all runs for the expulsion period. The results of this analysis are included with the tabular data in tables I and II.

RESULTS AND DISCUSSION

The main parameter used to compare the effectiveness of the various operating parameters on the amount of pressurant gas used is the nondimensional ratio M_I/M_G, where M_I is the ideal pressurant required to pressurize or expel a given volume of liquid at a given inlet gas temperature and tank pressure. The actual pressurant requirement for the same conditions is M_G. A higher M_I/M_G ratio means less energy and mass exchange. It does not necessarily mean a lower absolute pressurant requirement M_G as will be illustrated later in this section.

A value of 1 for M_I/M_G implies that there is no heat transferred to the tank wall or liquid and no mass transfer. This in turn implies that for no environmental heating the terms $\Delta U_W/\Delta U_T$ and $\Delta U_L/\Delta U_T$ in equation (22) are zero and that $\Delta U_U/\Delta U_T$ is equal to 1; that is, all the energy added to the tank during expulsion (ΔU_T) appears as an increase in ullage energy (ΔU_U). Therefore, any value of M_I/M_G or $\Delta U_U/\Delta U_T$ less than 1 means energy is lost by the ullage system. This loss of ullage energy would then appear as an increase in tank wall heating and/or liquid heating ($\Delta U_W/\Delta U_T$ and/or $\Delta U_L/\Delta U_T$).

The discussion of results will first present the effects of the various operating parameters on the ratio M_I/M_G, which was of primary interest, followed by mass transfer M_t/M_G results. Then the results of the energy balances will be presented in an attempt to point out major reasons for the ratios M_I/M_G or $\Delta U_U/\Delta U_T$ being less than 1. Finally, a comparison will be made between the experimental results and the analytically predicted results in order to determine the validity of the analytical program. The analytical results are presented in the figures along with the corresponding experimental results. The comparison between experimental and analytical results will be given in terms of an average deviation, which is defined as

$$\left[\frac{\sum_{N} \frac{\left|(\text{Experimental ratio}) - (\text{Analytical ratio})\right|}{(\text{Experimental ratio})}}{N}\right](100) \qquad (23)$$

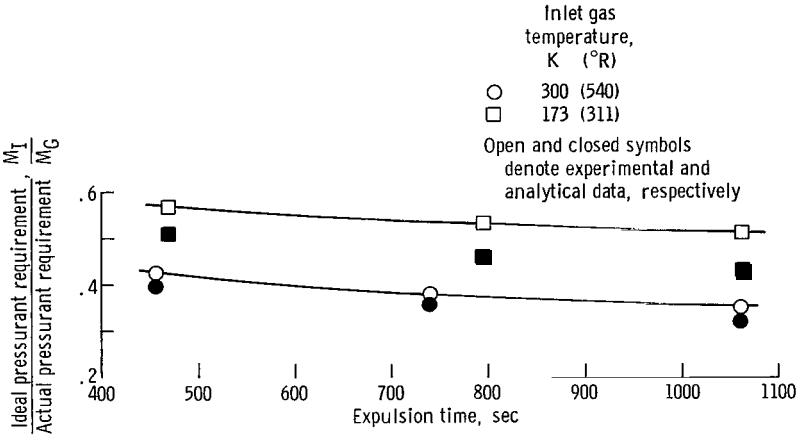

Figure 7. - Comparison of ideal pressurant requirement to actual pressurant requirement ratio for various expulsion times for two inlet gas temperatures. Hemisphere injector; tank pressure, 34.47×10^4 newtons per square meter (50 psia).

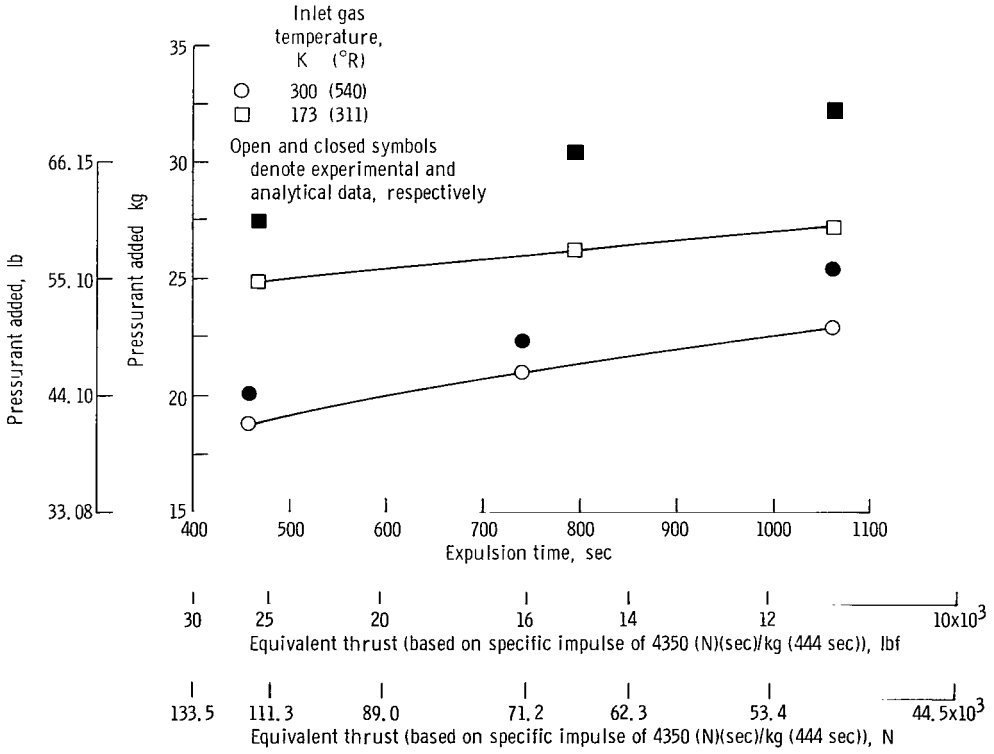

Figure 8. - Comparison of actual pressurant requirements for various expulsion times for two inlet gas temperatures. Hemisphere injector; tank pressure, 34.47×10^4 newtons per square meter (50 psia).

TABLE III. - DEVIATIONS BETWEEN EXPERIMENTAL AND ANALYTICAL RESULTS

Run	Injector	Inlet gas temperature		Tank pressure, N/m^2	Percent deviation between experimental and analytical results[a]			
		K	^oR		M_I/M_G	$\Delta U_U/\Delta U_T$	$\Delta U_w/\Delta U_T$	$\Delta U_L/\Delta U_T$
18	Hemisphere	300	540	34.47×10^4	+9.85	-10.50	+8.30	+4.11
19	↓	298	536	↓	+6.08	-16.27	+6.59	+23.37
20		298	536		+6.83	-22.81	+3.88	+12.24
25		173	311		+15.84	-16.17	+21.90	+13.92
26		172	310		+14.04	-17.79	+17.25	+26.66
27	↓	170	106	↓	+10.24	-24.05	+8.08	+15.78
30	Straight pipe	292	526	34.47×10^4	+43.83	+23.82	+1.80	+39.04
31	Straight pipe	292	526	34.47×10^4	+44.93	+26.78	-15.20	+57.07
34	Hemisphere	290	522	51.71×10^4	+16.78	-11.76	+8.64	-3.65
35	↓	↓	↓	↓	+15.47	-32.01	-4.21	+29.29
37					+1.82	-34.51	-7.06	+8.41
39		285	513	24.13×10^4	+14.19	-5.30	+11.41	+14.29
40		286	515	↓	+13.05	-11.11	+10.97	+6.76
42	↓	286	515		+14.18	-15.56	+6.75	0

[a]Analysis underpredicts, +; analysis overpredicts, -.

where N is the number of data points in a given set of operating conditions (i.e., when a hemisphere injector is used for a constant inlet gas temperature of 173 K (311^o R), N would be 3 for data presented in figs. 7 and 8). For convenience, individual deviations between the experimental and analytical results are summarized in table III.

The operating parameters, inlet gas temperature, injector geometry, tank pressure and outflow rates, as well as major experimental and analytical results, are summarized in tables I and II. Table I gives experimental and analytical mass balance results while table II gives the corresponding energy balance results.

Temperature Effect Using a Distributing Injector (Hemisphere)

Pressurant Requirements

The effect of two inlet gas temperatures is compared in figure 7 on the basis of M_I/M_G for various expulsion times. Expulsion time is the total time required to expel liquid from a 5-percent ullage to a 95-percent ullage. Therefore, each data point rep-

resents a complete expulsion. As can be seen in the figure, the ratio M_I/M_G is lower for the higher inlet gas temperature. This implies a larger percentage of energy that is contained in the pressurant gas is lost to the tank wall and liquid as the inlet gas temperature is increased. The average decrease in M_I/M_G for all expulsion times in going from 173 K (311° R) inlet gas temperature to a 300 K (540° R) inlet temperature is 29.0 percent. A comparison of the actual pressurant requirements M_G for the two inlet gas temperatures for various expulsion times is shown in figure 8. For reference, the various expulsion times (or constant liquid outflow rates) are also shown in terms of an equivalent thrust level based on the specific impulse of the RL10A3-3 engine (4350 (N)(sec)/(kg); 444 sec). The actual pressurant requirements M_G decrease for increasing inlet gas temperature, and increase for increasing expulsion times. Although the absolute value of M_G decreases for increasing inlet gas temperatures, the ratio M_I/M_G also decreases because of the even greater decrease in ideal requirements.

The shaded symbols in figures 7 and 8 are the results as predicted by the analytical program. The analysis underpredicts the M_I/M_G ratio (overpredicts M_G) by an average of 7.59 percent for the 300 K (540° R) inlet gas temperature and 13.37 percent for the 173 K (311° R) inlet gas temperature (see table III for actual deviations).

Mass transfer. - A comparison of the ratio of mass transferred during expulsion to the actual pressurant added to the tank M_t/M_G for different expulsion times and the two inlet gas temperatures is presented in figure 9. In all cases, the net mass transfer was condensation and represented between 2.9 and 8.3 percent of the pressurant mass added to the tank during expulsion. For a given inlet gas temperature, the ratio M_t/M_G decreases for increasing expulsion time. And for a given expulsion time, the ratio was higher for the higher inlet gas temperature with the exception of the 1060-second run

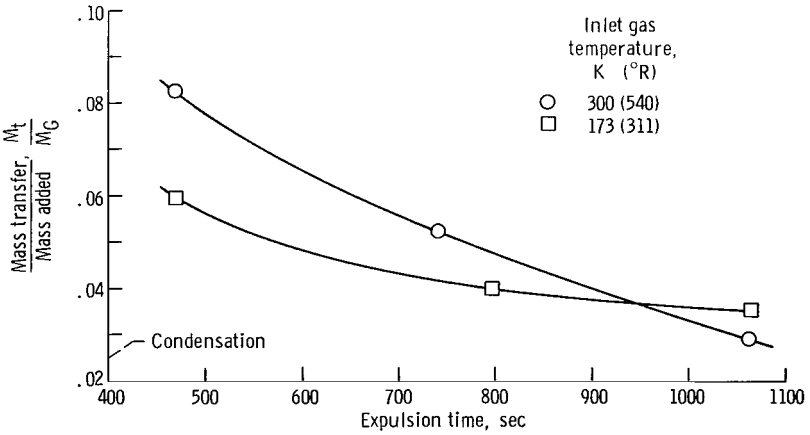

Figure 9. - Comparison of mass transfer to mass added ratio for various expulsion times for two inlet gas temperatures. Hemisphere injector; tank pressure, 34.47×10^4 newtons per square meter (50 psia).

where the 300 K (540° R) inlet gas produced less condensation (lower M_t/M_G) than the 173 K (311° R) inlet gas.

The results of reference 4 (which deal with a 1.52-m-diam spherical tank) indicate the major mode of mass transfer to be evaporation, whereas these tests (3.96-m-diam spherical tank) indicate condensation for similar test conditions. A possible reason for this reversal in the mass transfer mode is the difference in the gas velocities in the vicinity of the liquid surface during the expulsion. Based on the open area of the hemisphere injectors used in both tanks (928 cm^2 for the hemisphere used in the 3.96-m-diam tank and 174 cm^2 for the 1.52-m-diam tank) and the measured pressurant flow rates for the shortest expulsion times (457 sec for the 3.96-m tank and 132 sec for the 1.52-m tank), the gas velocity at the injector outlet for the 3.96-meter tank is approximately the same as that obtained in the 1.52-meter tank. However, the liquid surface, in the 3.96-meter tank, is 2.6 times farther from the injector than it is in the 1.52-meter tank. Thus, the velocity of the gas at the liquid surface would be reduced, leading to reduced impingement of the pressurant gas stream into the liquid surface. The authors believe that this reduced impingement results in gas condensation for the 3.96-meter-diameter tank.

The trend for both tanks for increasing expulsion times is toward evaporation. The limiting condition (as expulsion time $\rightarrow \infty$) would be the boiloff due to external heat input.

Energy remaining in ullage. - The ratios of the energy increase in the ullage over the expulsion period to the total energy added to the system $\Delta U_U/\Delta U_T$ for different expulsion times are compared in figure 10 for the two inlet gas temperatures. For all runs, between 27.5 and 50 percent of the total energy added to the system remains in the ullage after expulsion. For any given expulsion time, the ratio $\Delta U_U/\Delta U_T$ decreases for increasing inlet gas temperatures. Also, for a given inlet gas temperature, the

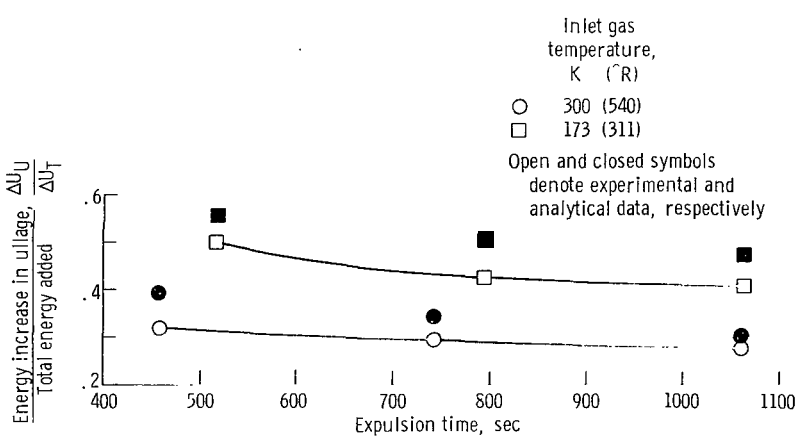

Figure 10. - Comparison of energy increase in ullage to total energy added ratio for various expulsion times for two inlet gas temperatures. Hemisphere injector; tank pressure, 34.47×10^4 newtons per square meter (50 psia).

ratio $\Delta U_U/\Delta U_T$ decreases with increasing expulsion time. It should be noted that the absolute value of ΔU_U does not change significantly for the two operating inlet gas temperatures used during testing. The mean increase in ullage energy for these series of runs (table II) was 27.7×10^6 joules (26 287 Btu) with a standard deviation of 1.23×10^6 joules (1165 Btu). Any trends in the ratio $\Delta U_U/\Delta U_T$, therefore, depend mainly on variations in the total energy added (ΔU_T) to the system because of variations in energy losses to the tank wall and liquid.

The analysis overpredicts $\Delta U_U/\Delta U_T$ by an average of 19.3 percent for inlet gas temperatures of 173 K (311° R) and by an average of 16.5 percent for an inlet gas temperature of 300 K (540° R).

Energy added to tank wall. - The ratio of energy gained by the tank wall to the total energy added to the system $\Delta U_W/\Delta U_T$ for different expulsion times is compared in figure 11 for two inlet gas temperatures. In general, between 35.9 and 57.9 percent of the

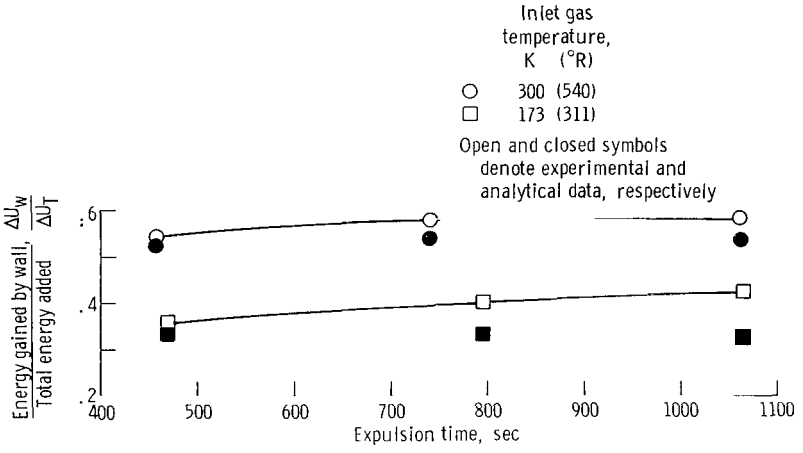

Figure 11. - Comparison of energy gained by wall to total energy added ratio for various expulsion times using two inlet gas temperatures. Hemisphere injector; tank pressure, 34.47×10^4 newtons per square meter (50 psia).

total energy added to the system was gained by the tank wall over the range of conditions. As can be seen in table II and in figure 11, both the absolute value of ΔU_W and the ratio $\Delta U_W/\Delta U_T$ increase with increasing inlet gas temperature. The increase in ΔU_W is due to the larger driving potential ΔT for heat transfer between the ullage gas and the tank wall. The total energy added to the tank ΔU_T does not increase in the same proportion as ΔU_W, which results in the increasing ratio $\Delta U_W/\Delta U_T$. The flatness of the two curves indicates that ΔU_W and ΔU_T increase in approximately the same proportion with increasing expulsion time. The analysis underpredicts the $\Delta U_W/\Delta U_T$ ratio by

an average of 6.3 and 15.7 percent for the 300 and 173 K (540° and 311° R) inlet gas temperature, respectively.

The results of reference 4 showed that between 30 and 58.8 percent of the total energy added to the tank was gained by the tank wall over similar test conditions. In these two cases, tank size has a relatively small effect on the percent of total energy gained by the tank wall.

Energy gained by liquid. - Figure 12 is a comparison of the ratio of energy gained by the liquid to the total energy added to the tank $\Delta U_L/\Delta U_T$ for different expulsion times for the two inlet gas temperatures. In all cases, between 10 and 24 percent of the total energy added to the tank appears as an increase of liquid energy (liquid heating).

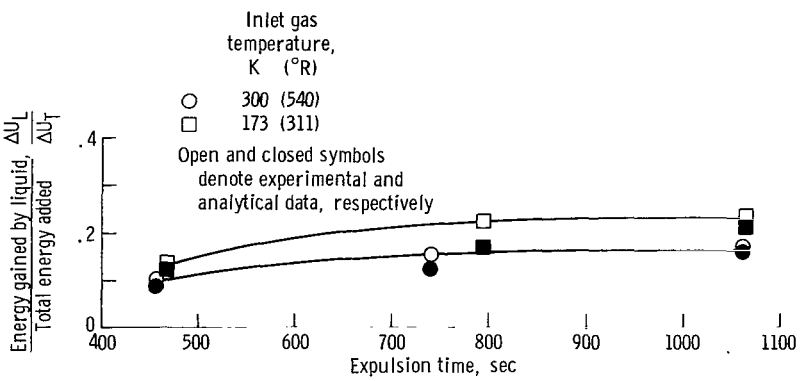

Figure 12. - Comparison of energy gained by liquid to total energy added ratio for various expulsion times for two inlet gas temperatures. Hemisphere injector; tank pressure, 34.47×10^4 newtons per square meter (50 psia).

The experimental data indicate a decreasing $\Delta U_L/\Delta U_T$ ratio for increasing inlet gas temperatures although the absolute magnitude of energy gained by the liquid is approximately the same for both inlet gas temperatures at comparable expulsion times (see table II). The decreasing $\Delta U_L/\Delta U_T$ is therefore due to increased total energy required ΔU_T when using the higher inlet gas temperature. The data also indicate increasing ΔU_L and $\Delta U_L/\Delta U_T$ for increasing expulsion times for a given inlet gas temperature. The increase in ΔU_L is the result of the longer exposure of the liquid surface to a heat source.

The analytical predictions of the ratio $\Delta U_L/\Delta U_T$ are also presented in figure 12 (see table III for average deviations). The large discrepancy between analysis and experimental data is partly caused by the error in experimentally determining the gain in liquid energy ΔU_L. The probable error associated with experimental determination of ΔU_L is between 10 and 17 percent (see table II). The analytical trend, however, is the same as observed experimentally; that is, the analysis predicts decreasing $\Delta U_L/\Delta U_T$

with increasing inlet gas temperature for constant expulsion time and increasing $\Delta U_L/\Delta U_T$ with increasing expulsion time for a constant inlet temperature.

Temperature distributions. - The results from the previous discussion point out that in all cases between 82.5 and 90 percent of the total energy that was added to the system is either absorbed by the tank wall or remains in the ullage. The correlation between the analysis and experimental data, therefore, depends largely on the ability of the analysis to predict final wall and ullage gas temperature profiles. These temperature profiles are, in turn, used to determine the increase in wall and ullage energy and the final ullage mass. The ability to predict these temperatures explains the good agreement between the experimental data and analysis reported in references 1 and 4.

To verify this agreement for the tests with the 3.96-meter tank, figures 13 and 14 present comparisons of experimental and analytical wall and ullage gas temperature profiles resulting from the two inlet gas temperatures.

Figure 13 presents a comparison of experimental and analytical wall and ullage gas temperature profiles at the end of a 740-second expulsion for a run which had an inlet gas temperature of 300 K (540° R). For this run, the ratios M_I/M_G and $\Delta U_w/\Delta U_T$ predicted by the analysis were within 6.08 and 6.59 percent of the experimental results (see table III). The experimental gas temperatures shown in figure 13 are obtained from

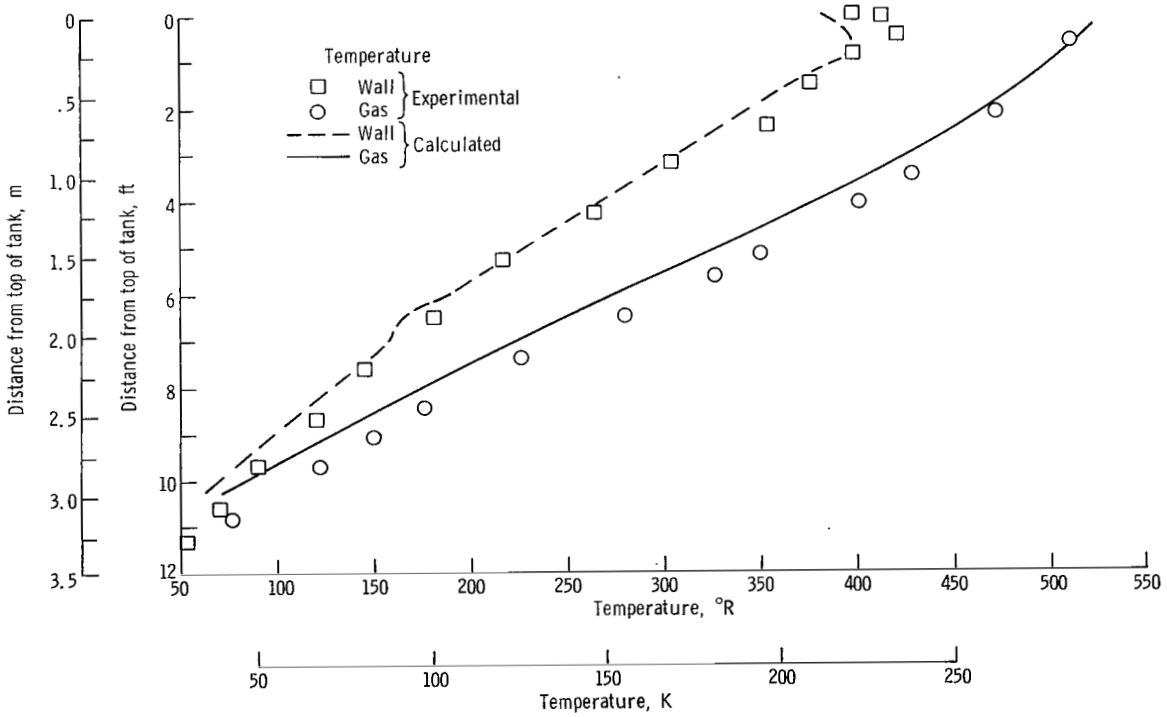

Figure 13. - Comparison of calculated and experimental gas and wall temperature profiles at end of 740-second expulsion. Hemisphere injector; inlet gas temperature, ~300 K (540° R); tank pressure, 34.47×10^4 newtons per square meter (50 psia).

the vertical rake and indicate average radial temperatures at their respective vertical positions. In the absence of any mass transfer, the pressurant mass required for an expulsion could be determined as the difference between the final mass in the ullage and the initial mass prior to expulsion. Since one of the initial conditions for the analytical program is the initial experimental temperature profile (and, therefore, the initial ullage mass) prior to expulsion, the deviation in pressurant requirements would largely be the results of the predicted final temperature profile.

As seen in figure 13, the calculated final ullage gas temperatures are lower than the experimentally observed temperatures at every position in the tank. As a result, the final calculated ullage mass is greater than that determined experimentally and therefore leads to an underprediction of the M_I/M_G ratio.

The calculated wall temperatures are also lower than the experimentally observed temperatures. The slightly lower temperatures together with the fact that the specific heat of the wall is a strong function of temperature results in the 6.59-percent underprediction of the $\Delta U_W/\Delta U_T$ ratio.

Figure 14 presents a similar comparison of experimental and analytical wall and ullage gas temperature profiles at the end of a 795-second expulsion which had an inlet gas temperature of 173 K (311° R). Here the calculated final ullage gas temperatures

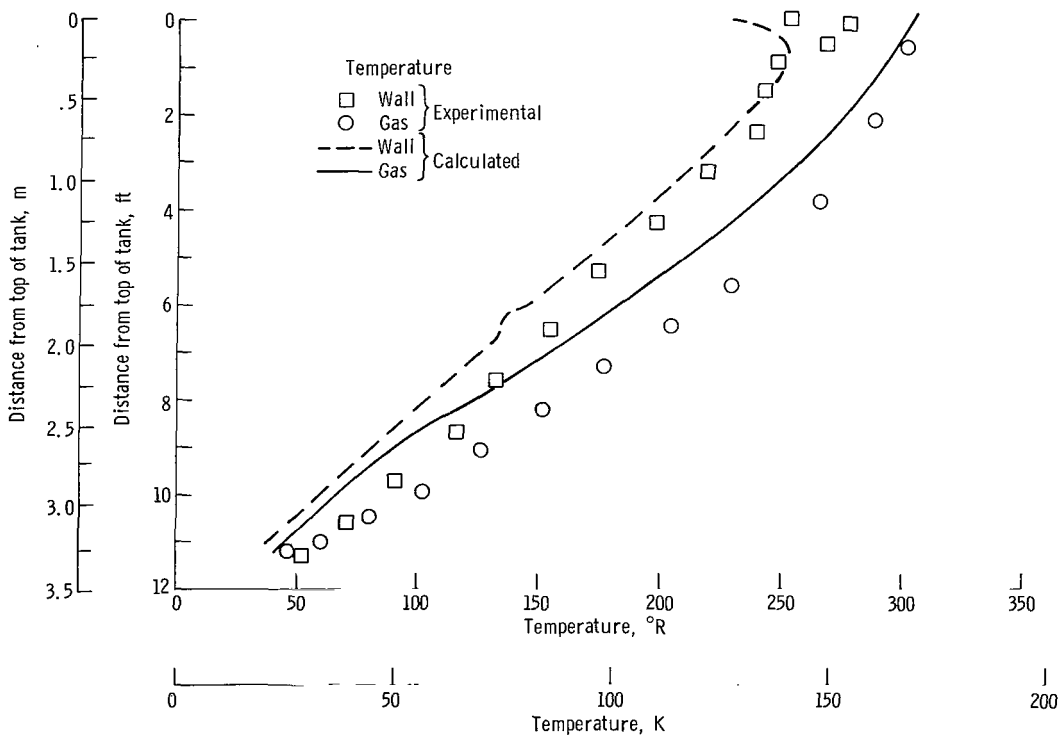

Figure 14. - Comparison of calculated and experimental gas and wall temperature profiles at end of 795-second expulsion. Hemisphere injector; inlet gas temperature, ~173 K (311° R); tank pressure, 34.47×10^4 newtons per square meter (50 psia).

are much lower than experimentally observed temperatures resulting in a large deviation (14.04 percent) between analysis and the observed value of pressurant requirements (M_I/M_G). The predicted wall temperatures are also lower than the temperatures observed experimentally. As a result, the analysis underpredicts tank wall heating $\Delta U_w/\Delta U_T$ by 17.25 percent.

The reasons for the larger deviations between analytical and experimental values for M_I/M_G and $\Delta U_w/\Delta U_T$ for the lower inlet gas temperature are not clearly understood.

Injector Effect

Pressurant requirements. - The effect of injector geometry on the pressurant requirements (M_I/M_G ratio) for different expulsion times for an inlet gas temperature of 294±6 K (529°±11° R) is shown in figure 15. The comparison is made between a straight pipe injector, which injects the pressurant gas in a concentrated jet toward the liquid, and a hemisphere injector (fig. 4), which diffuses the pressurant uniformly throughout the ullage volume. Data for the straight pipe injector were not reported for expulsion times lower than 780 seconds because of a tank pressure dropoff encountered at the beginning of the expulsion period. Tank pressure dropoffs from a nominal operating pressure of 34.47×10^4 newtons per square meter (50 psia) to values as low as 20.47×10^4 newtons per square meter (29 psia) were observed before the recovery of pressure back to the original operating level could be achieved by the control system. Similar type pressure dropoffs were reported in reference 3 while testing a straight pipe injector. These pressure dropoffs are attributed to rapid temperature decay in the ullage due to violent mixing of ullage gas and liquid droplets caused by direct impingement of pressurant gas into the liquid surface.

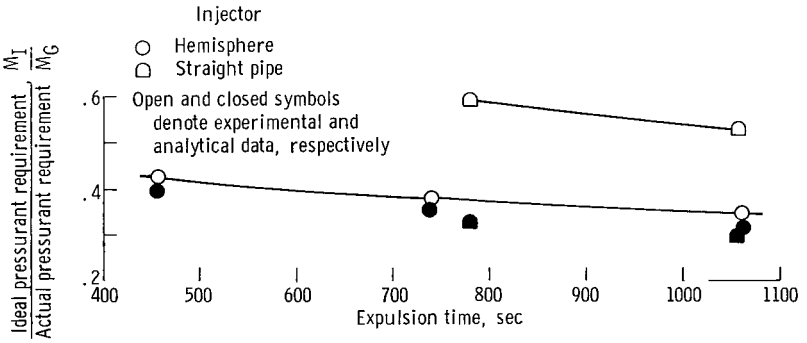

Figure 15. - Comparison of ideal pressurant requirement to actual pressurant requirement ratio for various expulsion times for two injector geometries. Inlet gas temperature, ~294±6 K (529°±11° R); tank pressure, 34.47×10^4 newtons per square meter (50 psia).

For the data obtained, the straight pipe has less pressurant requirements (greater M_I/M_G) than the hemisphere injector (similar results were obtained in ref. 4). The straight pipe has a 35.0 percent lower pressurant requirement (greater M_I/M_G) for a 780-second expulsion and a 32.4 percent lower requirement for a 1052-second expulsion. The reasons for the decreased pressurant (as will be discussed later in this section) are (1) less energy transfer to the tank wall and (2) evaporation of liquid. Both injector types indicate increasing pressurant requirements (decreasing M_I/M_G) for increasing expulsion times. The analytical predictions of pressurant requirements M_I/M_G are also presented in figure 15 (see table III for deviations).

A basic assumption of the analytical model is that of one-dimensional flow. References 3 and 4 both indicate that this assumption is valid when using injectors that diffuse the pressurant throughout the ullage but is not valid when using a straight pipe injector. Similar results are evident for these tests. Since the analytical program does not distinguish variations in injection pattern, its results for both injectors can be approximated by a single curve.

Mass transfer. - The comparison of the M_t/M_G ratio for different expulsion times for the two injectors is shown in figure 16. The M_t/M_G ratio (always condensa-

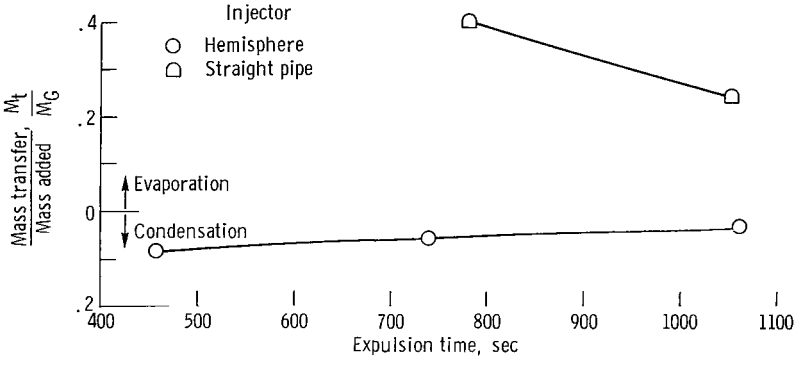

Figure 16. - Comparison of mass transfer to mass added ratio for various expulsion times for two injector geometries. Inlet gas temperature, 294±6 K (529°±11° R); tank pressure, 34.47x10^4 newtons per square meter (50 psia).

tion) for the hemisphere injector was discussed previously. The mode of mass transfer when using the straight pipe injector was evaporation. This evaporation is caused by a forceful impingement of the pressurant gas stream into the liquid surface. The inlet velocity of the pressurant gas decreases for increasing expulsion times resulting in reduced impingement and reduced evaporation (decreasing M_t/M_G).

Energy remaining in ullage. - The comparison of the $\Delta U_U/\Delta U_T$ ratio for different expulsion times for the two injector geometries is shown in figure 17. As stated pre-

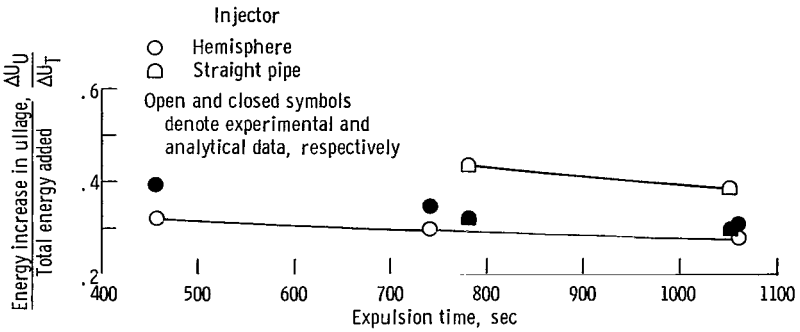

Figure 17. - Comparison of energy increase in ullage to total energy added ratio for various expulsion times for two injector geometries. Inlet gas temperature, 294±6 K (529°±11° R); tank pressure, 34.47×10^4 newtons per square meter (50 psia).

viously, between 27.5 and 32 percent of the total energy added to the tank remains in the ullage at the end of expulsion when using the hemisphere injector. For the straight pipe injector between 38.2 and 43.3 percent remains in the ullage. There is an average of 45.7 percent more energy remaining in the ullage than the hemisphere injector indicated. This means less pressurant energy was lost to the tank wall and liquid while using the straight pipe injector. Both injectors show a decreasing $\Delta U_U/\Delta U_T$ ratio for increasing expulsion times, which indicates more pressurant energy was lost to tank wall and/or liquid because of a longer exposure to the cold environment. The analysis overpredicts the energy remaining in the ullage $\Delta U_U/\Delta U_T$ by an average of 16.53 percent for the hemisphere, but it underpredicts that quantity by an average of 19.34 percent for the straight pipe injector. This 19.34 percent underprediction will be discussed later in this section.

Energy added to tank wall. - The ratio of energy gained by the tank wall to the total energy added to the tank $\Delta U_W/\Delta U_T$ for different expulsion times for the two injector

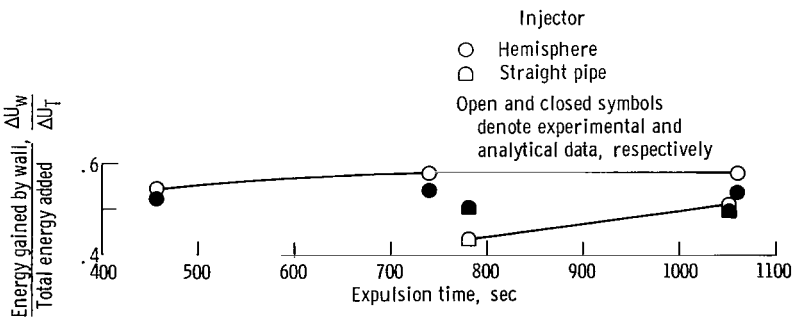

Figure 18. - Comparison of energy gained by wall to total energy added ratio for various expulsion times for two injector geometries. Inlet gas temperature, 294±6 K (529°±11° R); tank pressure, 34.47×10^4 newtons per square meter (50 psia).

geometries is shown in figure 18. The straight pipe injector has less wall heating (lower $\Delta U_w/\Delta U_T$) than the hemisphere types - 25.9 percent lower at a 780-second expulsion and 13.8 percent lower at a 1052-second expulsion. As mentioned previously, the ratio $\Delta U_w/\Delta U_T$ is relatively independent of expulsion time for the hemisphere injector, whereas $\Delta U_w/\Delta U_T$ increases for increasing expulsion time when using the straight pipe injector. The reduced wall heating when using the straight pipe is due to lower, nearly constant, axial temperatures in the upper portion of the ullage together with rather large radial temperature gradients that were lowest near the tank wall and

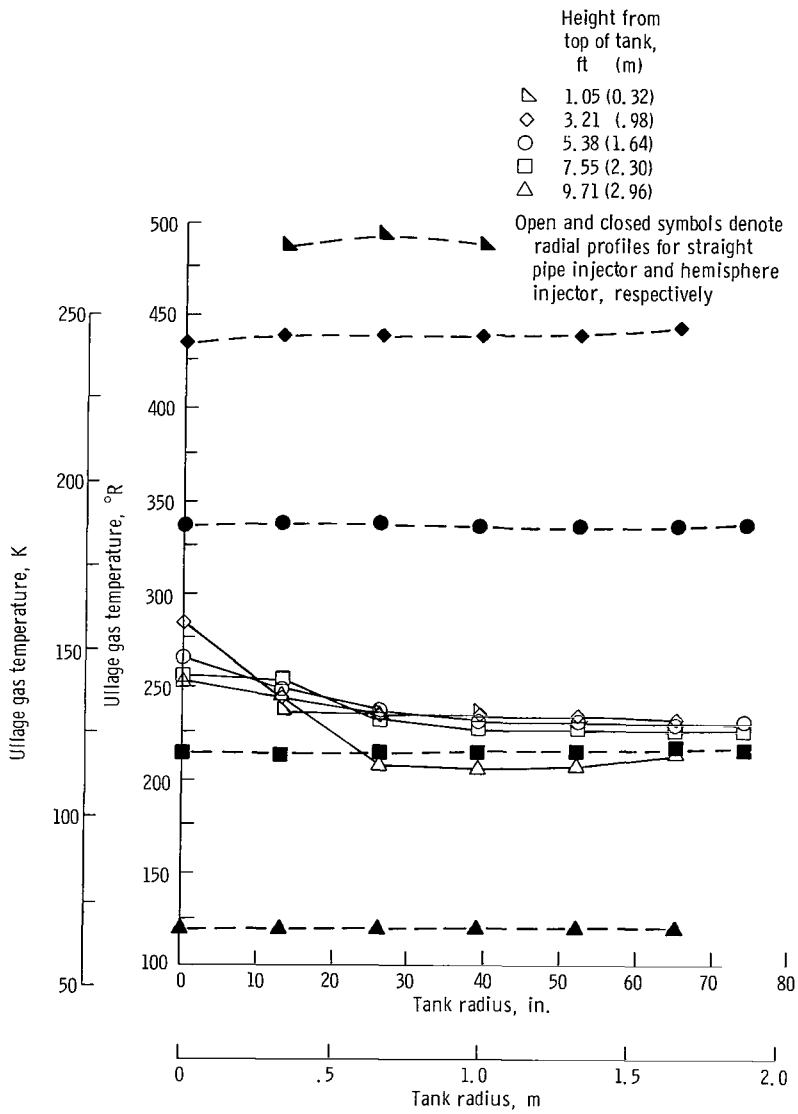

Figure 19. - Comparison of radial gas temperature profiles obtained at end of 780-second expulsion for straight pipe and hemisphere injector. Inlet gas temperature, ~294 K (529° R).

highest at the center of the tank. The constant axial temperature will be discussed later in this section. The measured variations in radial ullage gas temperature profiles for the straight pipe injector (at the end of a 780-sec expulsion) and the hemisphere injector (at the end of a 740-sec expulsion) for approximately the same inlet gas temperature are shown in figure 19.

The analysis overpredicts $\Delta U_W/\Delta U_T$ when using the straight pipe injector by an average of 8.50 percent. This ratio for the straight pipe is misleading because of the large overprediction of pressurant requirements. The overprediction on pressurant requirements results in a large overprediction of the total energy added (ΔU_T). The actual deviations between analytically and experimentally determined wall energy increase ΔU_W are 82.5 and 52.0 percent, respectively. This overprediction will be discussed in the temperature distribution section.

Energy gained by liquid. - Figure 20 presents a comparison of the $\Delta U_L/\Delta U_T$ ratio for different expulsion times for the two injector geometries. Between 10 and 17 percent of the total energy added to the tank appears as an increase in liquid energy when using the hemisphere injector. The straight pipe injector produces a larger amount of liquid heating: Between 35.6 and 42.5 percent of the total energy added to the tank appears as an increase in liquid energy. The hemisphere injector produces increased liquid heating (increased $\Delta U_L/\Delta U_T$) for increasing expulsion time, whereas the straight pipe produces decreased liquid heating (decreased $\Delta U_L/\Delta U_T$) for increasing expulsion. Based on the slopes of the two curves shown in figure 20, it appears that at some expulsion greater than 1100 seconds the hemisphere and straight pipe injectors would produce the same amount of liquid heating (a similar observation can be made for the mass transferred, see fig. 16). At this point, the effect of the injection pattern of the straight pipe would be minimized because of the low injection velocities.

Here again the analytical data for both injectors can be approximated by a single

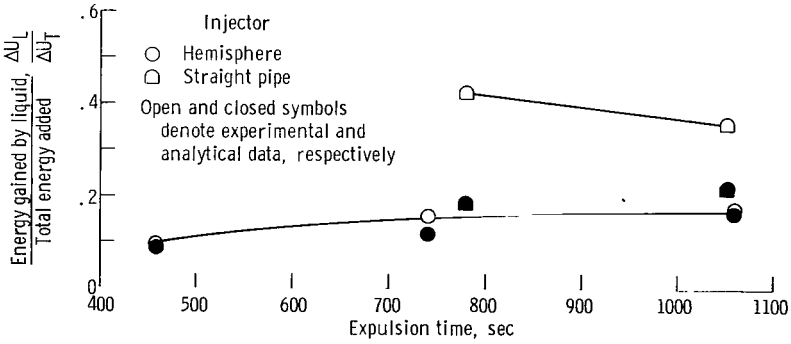

Figure 20. - Comparison of energy gained by liquid to total energy added ratio for various expulsion times for two injector geometries. Inlet gas temperature, 294±6 K (529°±11° R); tank pressure, 34.47x10^4 newtons per square meter (50 psia).

curve because of the inability of the program to distinguish injector variations. As a result, the predictions are good for the hemisphere injector and poor for the straight pipe injector. The scatter that is present in the analytical data is the result of variations in initial conditions (e.g., initial wall and gas temperature profiles and inlet gas temperature and pressure) for the different injectors.

Temperature distribution. - Figure 21 compares experimental and calculated gas and wall temperature profiles for the straight pipe injector at the end of a 780-second expulsion. The comparison of wall and gas profiles for the hemisphere was made previously. The experimental data show a nearly constant ullage temperature profile in the upper 60 percent of the ullage and then a decrease almost linearly to the liquid surface. The experimental wall temperature profile is similar to that of the ullage. The analytical gas temperatures increase almost linearly from the liquid surface to the top of the tank. The large differences in analytical and experimental final ullage gas temperature profiles result in a large deviation in the predicted value of pressurant requirement M_I/M_G (see table III). The analysis underpredicts the wall temperatures in the lower 54 percent of the tank and overpredicts in the upper 46 percent of the tank. The larger overprediction of wall temperatures in the upper 46 percent of the tank coupled with the fact that the specific heat of aluminum increases rapidly with increasing temperature

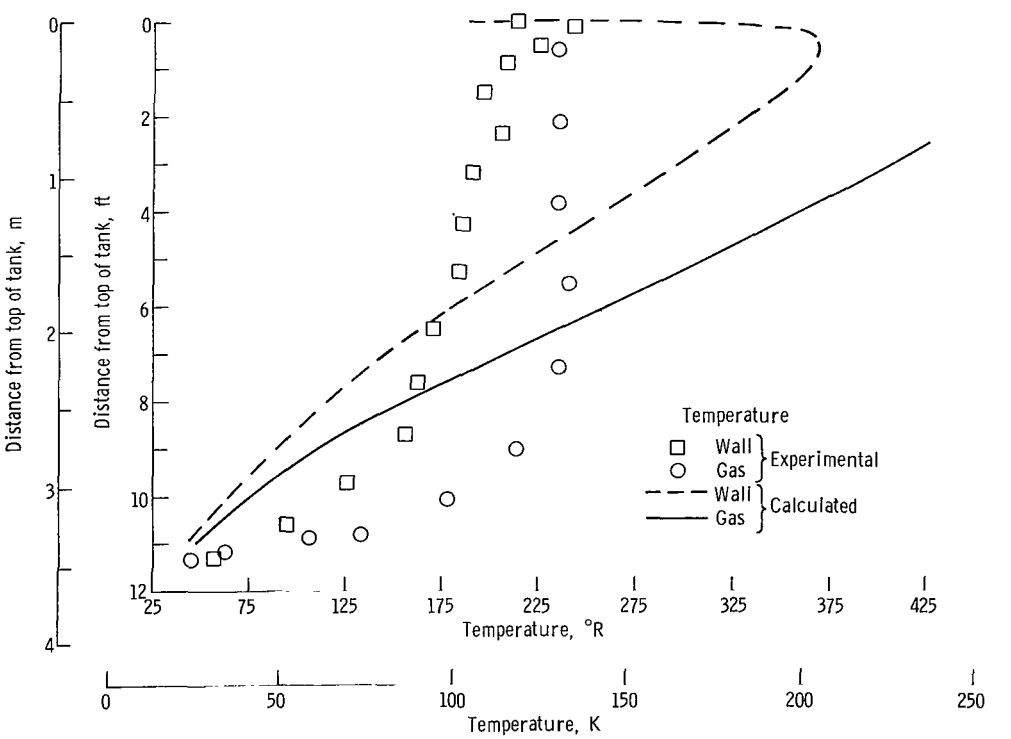

Figure 21. - Comparison of calculated and experimental gas and wall temperature profiles at end of 781-second expulsion. Straight pipe injector; inlet gas temperature, 291 K (524° R); tank pressure, 34.47×10^4 newtons per square meter (50 psia).

leads to the overprediction of 82.5 percent on ΔU_w. The analysis does not (with the present assumptions) have the capability to accurately predict either the gas or wall temperature profiles obtained when using the straight pipe injector.

Effect of Tank Pressure Level on Pressurant Requirements

A comparison of the pressurant requirements (M_I/M_G ratio) for different expulsion times for three tank pressure levels is presented in figure 22. The data presented in figure 22 were obtained using the hemisphere injector and an inlet gas temperature of 291±8 K (524°±14° R). The ratio M_I/M_G for the three tank pressure levels can be represented by a single curve which indicates that the actual pressurant requirements

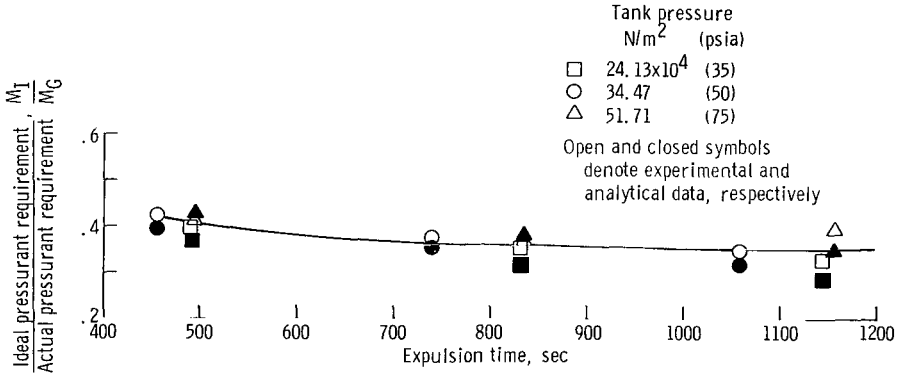

Figure 22. - Comparison of ideal pressurant requirement to actual pressurant requirement ratio for various expulsion times for three tank pressures. Hemisphere injector; inlet gas temperature, 291±8 K (524° ±14° R).

as well as ideal pressurant requirements (see eq. (2)) are directly proportional to tank pressure. The general trend is toward increasing pressurant requirements (decreasing M_I/M_G for increasing expulsion times for all tank pressure levels.

The agreement between the analysis and experimental results is good for the three tank pressure levels.

Mass transfer. - Figure 23 presents a comparison of mass transfer (M_t/M_G ratio) for different expulsion times for the three tank pressure levels. In all cases the net mode of mass transfer was condensation. For a given expulsion time there is increased condensation (increased M_t/M_G) for increased tank pressure levels. For increased expulsion times, there is decreased condensation (decreased M_t/M_G) for the three tank pressure levels.

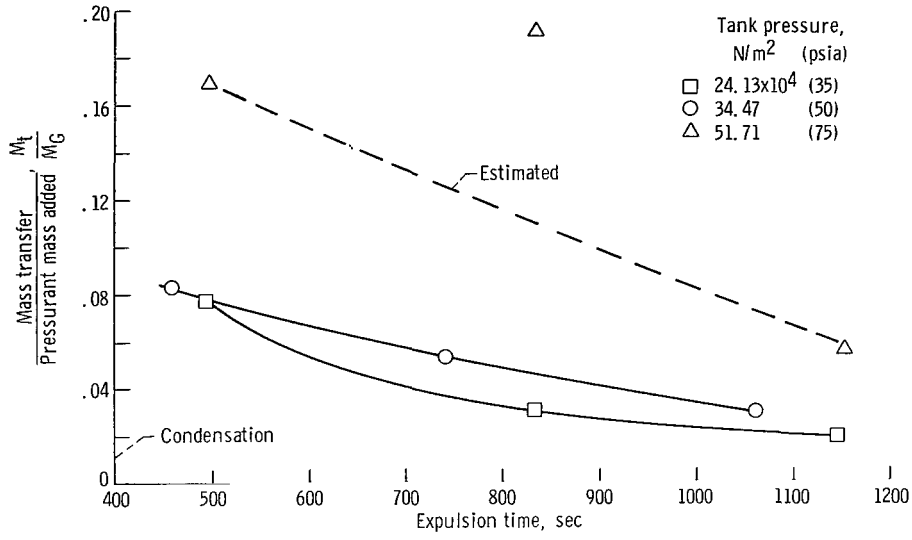

Figure 23. - Comparison of mass transfer to pressurant mass added ratio for various expulsion times for three tank pressures. Hemisphere injector; inlet gas temperature, 291±8 K (524°±14° R)

Energy remaining in ullage. - The ratios of the energy increase in the ullage during the expulsion period to the total energy added to the system ($\Delta U_U/\Delta U_T$) for different expulsion times are compared in figure 24 for the three tank pressure levels. Here again the experimental data for the three pressure levels can be represented by a single curve indicating that the ratio $\Delta U_U/\Delta U_T$ does not depend on tank pressure level. For a given expulsion time the same percentage of the total energy added to the tank is lost to the tank wall and/or liquid surface regardless of the tank pressure level. The trend is toward decreasing $\Delta U_U/\Delta U_T$ ratio for increasing expulsion time for all three tank pressures.

The average deviation between analytical and experimental results increases for increasing tank pressure level.

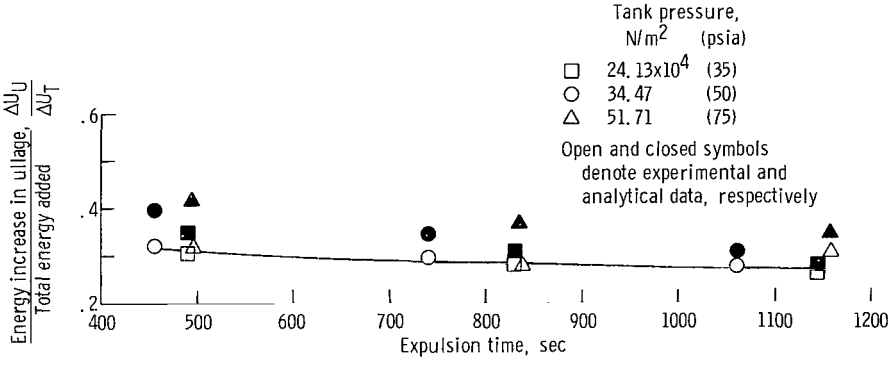

Figure 24. - Comparison of energy increase in ullage to total energy added ratio for various expulsion times for three tank pressures. Hemisphere injector; inlet gas temperature, 291±8 K (524°±14° R).

Energy added to tank wall. - The comparisons of the $\Delta U_W/\Delta U_T$ ratio for different expulsion times for the three tank pressure levels are presented in figure 25. The ratio $\Delta U_W/\Delta U_T$ decreases for increased tank pressure levels. There is an average decrease of 6.78 percent in $\Delta U_W/\Delta U_T$ going from a tank pressure of 24.13×10^4 to 34.47×10^4 newtons per square meter (35 to 50 psia) and an average decrease of 14.55 percent going from 34.47×10^4 to 51.71×10^4 newtons per square meter (50 to 75 psia). The actual magnitude of energy lost to the tank wall (ΔU_W) increases for increased tank pressure

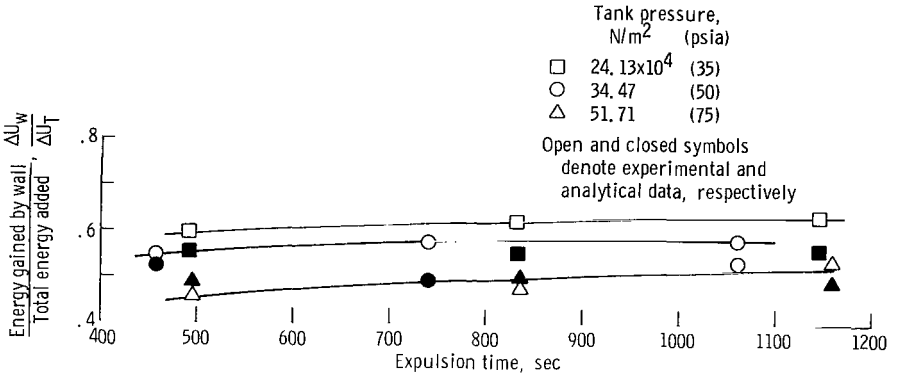

Figure 25. - Comparison of energy gained by wall to total energy added ratio for various expulsion times for three tank pressures. Hemisphere injector; inlet gas temperature, 291±8 K (524°±14° R).

levels. However, the total energy added to the system (ΔU_T) increased at a faster rate because of the higher inlet pressure, resulting in the decreased $\Delta U_W/\Delta U_T$ ratio for the higher pressure levels. In all cases the energy lost to the tank wall ($\Delta U_W/\Delta U_T$) increases for increasing expulsion time because of a longer exposure of the wall to a heat source.

The analysis underpredicts wall heating ($\Delta U_W/\Delta U_T$) in all but two cases.

Energy gained by liquid. - Figure 26 presents a comparison of the energy lost to the liquid ($\Delta U_L/\Delta U_T$) for different expulsion times at three tank pressures. There do not seem to be any identifiable trends in the ratio $\Delta U_L/\Delta U_T$ for various tank pressures even though the absolute value of energy lost to the liquid (ΔU_L) increases (at a given expulsion time) for increased tank pressures. In general, between 9.7 and 18.9 percent of the total energy added to the tank appears as an increase in liquid energy. Liquid heating increases with increasing expulsion time because of a longer exposure of the liquid to a heat source.

The analysis underpredicts liquid heating (ΔU_L) in all but one case. The large deviations may be the result of uncertainties of experimentally determining liquid heating (see table II).

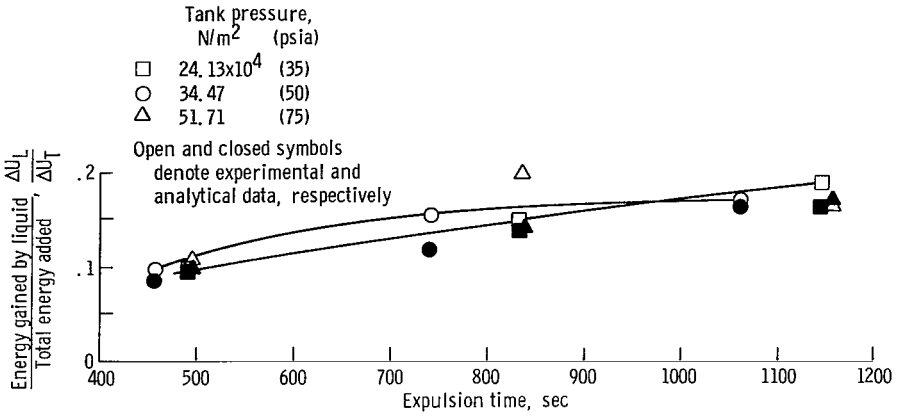

Figure 26. - Comparison of energy gained by liquid to total energy added ratio for various expulsion times for three tank pressures. Hemisphere injector; inlet gas temperature, 291±8 K (524°±14° R).

Temperature distribution. - In order to gain an insight into possible reasons for the deviation between analytical and experimental results, a comparison was made of experimental and calculated gas and wall temperature profiles for tank pressures of 24.13×10^4 and 51.71×10^4 newtons per square meter (35 and 75 psia; results of the 34.47×10^4 N/m^2 tank pressure tests were discussed previously). Figures 27 and 28 compared these temperature profiles at the end of approximately an 835-second expulsion, which represents an average expulsion time for this series of tests.

Figure 27 presents the temperature profiles for a run at a tank pressure of 24.13×10^4 newtons per square meter (35 psia) where the deviations between analytical and experimental results for U_W/U_T and M_I/M_G were 10.97 and 11.07 percent, respectively. The predicted ullage gas temperatures are lower than was observed experimentally. As a result, the final predicted ullage mass was greater resulting in an overprediction of 11.07 percent in pressurant requirements.

The analytically predicted wall temperatures (fig. 27) are also lower throughout the tank wall. The underprediction of temperatures of the tank wall result in the 10.97-percent underprediction of the ratio $\Delta U_W/\Delta U_T$.

Figure 28 presents the gas and wall temperature profiles for a 51.71×10^4 newtons per square meter (75 psia) tank pressure run where the deviations between analytical and experimental results for the ratios $\Delta U_W/\Delta U_T$ and M_I/M_G were 4.21 and 4.14 percent, respectively. The predicted ullage gas temperatures are again lower than the observed temperatures throughout the ullage volume. This fact in itself would indicate that the analytical program would overpredict the pressurant mass requirement. However, a large amount of condensation occurred for this run. As a result, the actual pressurant requirement increased to make up for the condensation. The predicted pressurant requirement was therefore 4.14 percent less than observed experimentally.

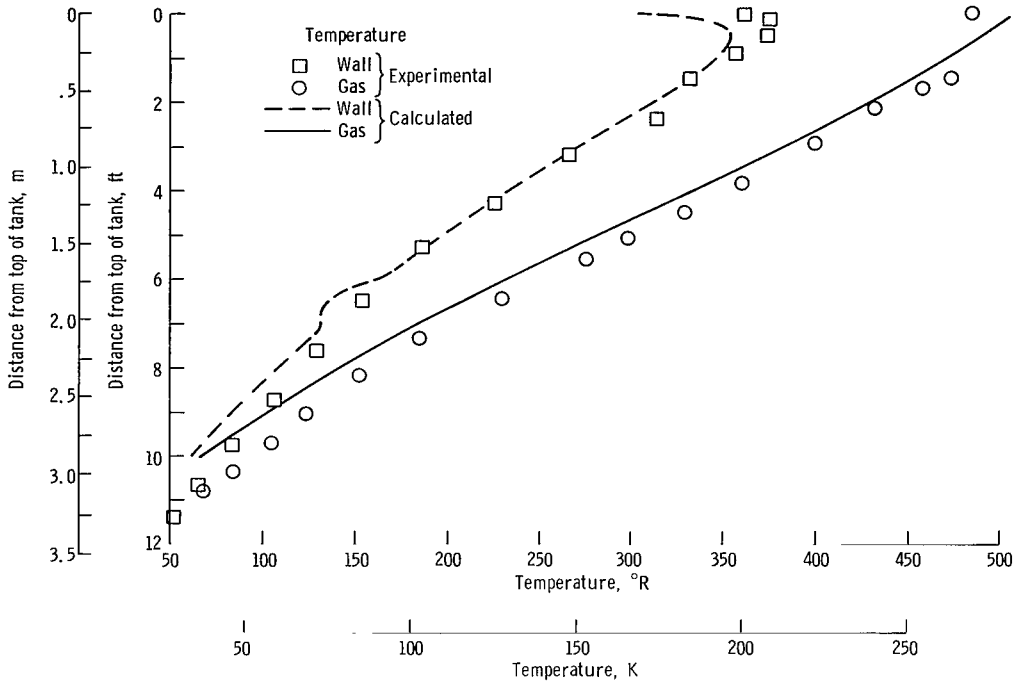

Figure 27. - Comparison of calculated and experimental gas and wall temperature profiles at end of 835-second expulsion. Hemisphere injector; inlet gas temperature, 286 K (515° R); tank pressure, 24.13×10^4 newtons per square meter (35 psia).

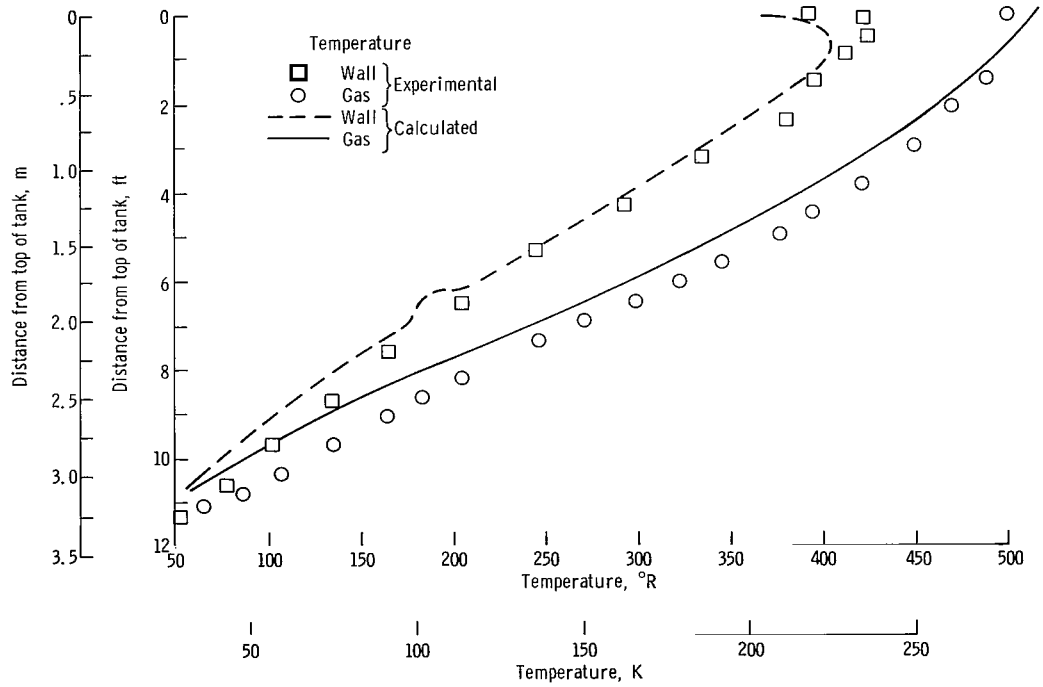

Figure 28. - Comparison of calculated and experimental gas and wall temperature profiles at end of 835-second expulsion. Hemisphere injector; inlet gas temperature, 289 K (520° R); tank pressure, 51.71×10^4 newtons per square meter (75 psia).

The analytically predicted wall temperatures (fig. 28) are lower than the observed temperatures throughout the tank. This underprediction of temperatures of the tank wall results in 16.2-percent underprediction of wall energy gain (ΔU_W). However, the analysis overpredicts the ratio $\Delta U_W/\Delta U_T$ by 4.21 percent because of the large underprediction of total energy added (ΔU_T). The large underprediction of total energy is the result of underpredicting the pressurant requirement as explained previously.

Effects of Ramp Rates on Pressurant Required to Pressurize the Tank at Various Initial Ullage Volumes

The amount of pressurant gas needed to initially pressurize a propellant tank may be important for certain missions. This is particularly true for multiburn missions where the tank is vented after each burn or where the coast period between firings is long enough to enable the ullage gas to collapse.

As stated in the INTRODUCTION, the purpose of this investigation was to determine the capability of the analysis to predict the pressurant requirements during the initial pressurization period as well as the expulsion period. For this purpose, data were collected during the initial pressurizing period for various pressurizing rates and ullage volumes.

Figure 29 is a comparison of pressurant mass requirements M_I/M_G as a function of ramp rate for various initial ullage volumes. This figure indicates decreased pressurant requirements (increased M_I/M_G) for increasing ramp rates for any given initial ullage volume. For the faster ramps, there is less time for the pressurant gas to lose energy to the surroundings. For any given ramp rate, the ratio M_I/M_G increases for larger initial ullage volumes probably because the initial wall temperature prior to ramp is higher for the larger ullage volume. Consequently, there is a smaller driving temperature between the ullage gas and tank wall, which results in reduced energy lost to the tank wall. The absolute pressurant requirements (both experimental and analytical) for the data presented in figure 29 are given in table IV.

The modification of the analysis of reference 1 for the ramp period is discussed in appendix C. As can be seen in figure 29, the analysis does not accurately predict the pressurant requirements during the pressurization of the 5-percent ullage (average deviation between analytical and experimental results is ±16.0 percent for 5-percent ullage). However, the prediction improves for the larger ullage volumes. The average deviation for the 26-, 52.5-, and 74-percent ullage volumes are ±4.6, ±3.7, and ±0.5 percent, respectively. This same analysis was used in reference 4 to predict the pressurant requirement during the initial pressurization period and was also found to be inadequate for the smaller ullage volumes.

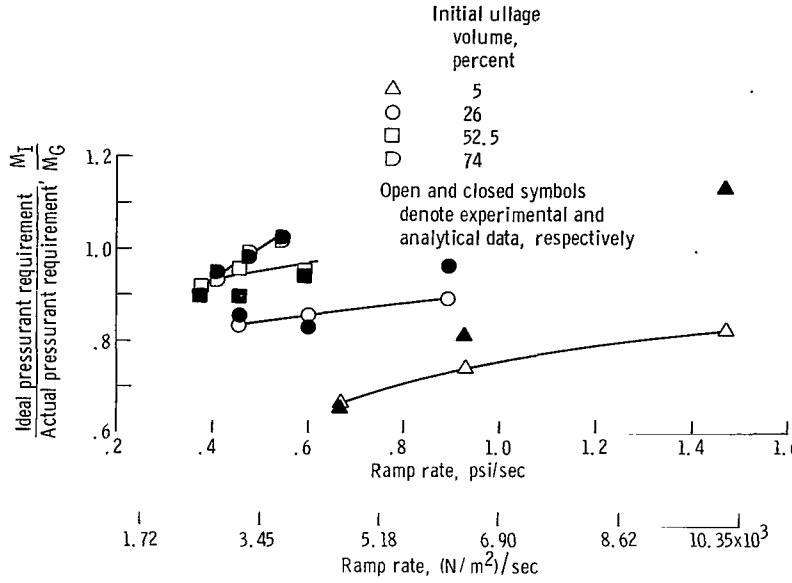

Figure 29. - Comparison of ideal pressurant requirement to actual pressurant requirement ratio as function of ramp rate for four initial ullage volumes. Hemisphere injector; inlet gas temperature, 167±8 K (301°±14° R).

TABLE IV. - COMPARISON OF EXPERIMENTAL AND ANALYTICAL VALUES OF PRESSURANT GAS REQUIREMENTS FOR RAMP PERIOD

Run	Initial ullage volume, percent	Ramp rate		Mass added				Inlet gas temperature	
		psi/sec	$(N/cm^2)/sec$	Experimental		Analytical			
				lb	kg	lb	kg	K	°R
23	5.0	0.668	0.461	1.084	0.492	1.088	0.494	176	316
24	5.0	.93	.641	1.082	.491	.982	.445	173	311
27	5.0	1.47	1.01	.945	.429	.687	.312	170	306
44	26.0	.893	.616	4.641	2.105	4.298	1.950	169.5	305
45	26.0	.599	.413	4.961	2.250	5.130	2.327	171	308
46	26.0	.454	.313	5.166	2.343	5.040	2.286	168	303
67	52.5	.59	.407	8.476	3.845	8.670	3.933	164	295
69	52.5	.456	.314	8.821	4.001	9.463	4.292	164	295
71	52.5	.376	.259	8.977	4.072	9.270	4.205	165.5	298
86	74.0	.544	.375	9.886	4.484	9.845	4.466	163	293
88	74.0	.475	.327	13.446	6.099	13.515	6.130	160	288
91	74.0	.409	.282	13.482	6.115	13.396	6.076	169.5	305

CONCLUDING REMARKS

The comparisons between the analytical and experimental results indicate that for the range of test conditions used, the analytical program and assumptions are adequate to allow prediction of gas requirements during the initial pressurization and expulsion periods when using a diffuser-type injector. However, the analytical results do not approach the experimental results when a straight pipe injector is used. This discrepancy is largely due to the fact that the analysis assumes stratified ullage gas with no radial temperature gradients. These assumptions are violated in the case of the straight pipe injector.

SUMMARY OF RESULTS

Tank pressurization and propellant expulsion tests were conducted in a 3.96-meter- (13-ft-) diameter spherical tank to determine the effect of various physical parameters on the pressurant gas requirements. The results obtained were compared with the results predicted by an analytical program. Tests were conducted using the two inlet gas temperatures, three tank pressure levels, two injector geometries, and various outflow rates. The results of this test program are now presented.

Experimental Results

The experimental results indicate a reduction of approximately 20 percent in pressurant gas requirements (M_G) for an increase in inlet gas temperature from 173 to 300 K (311° to 540° R). Increased inlet gas temperature decreases the residual mass and energy remaining in the ullage volume after expulsion. This decrease in residual energy results from an increase in total energy lost to the tank wall and liquid. Results indicate little difference in the absolute magnitude of mass transferred (M_t) but the mass transfer ratio (M_t/M_G) increased when the inlet gas temperature was increased.

The trends shown in this report for varying inlet gas temperatures are consistent with the results obtained in a 1.52-meter- (5-ft-) diameter spherical tank (ref. 4) with the exception of trends in the mass transfer ratio M_t/M_G. Reference 4 indicated increased evaporation for increasing inlet gas temperatures whereas this report indicates increased condensation.

Pressurized expulsion with the straight pipe injector requires approximately 34 percent less pressurant gas than with hemisphere injector. This reduced require-

ment is primarily the result of reduced tank wall heating (approximately 33 percent less) and of the evaporation of liquid hydrogen. The straight pipe injector increases liquid heating over that obtained with the hemisphere injector.

Operation at higher tank pressure levels increases the absolute value of pressurant mass required to expel a given volume of liquid. However, the tank pressure does not affect the ratio M_I/M_G; that is, for a 30-percent increase in tank pressure, both the actual pressurant requirement (M_G) and the ideal pressurant requirement (M_I) increase by approximately 30 percent. Both the absolute value of mass transfer (condensation) and the ratio M_t/M_G increase for increasing tank pressures. The absolute quantity of energy lost to the tank wall (ΔU_w) increases as the tank pressure is increased. However, the energy gained by the tank wall does not increase in the same proportion as the total energy added to the tank (ΔU_T). As a result, the ratio $\Delta U_w/\Delta U_T$ decreases for increased tank pressures. Both the absolute value of liquid energy gain ΔU_L and the ratio $\Delta U_L/\Delta U_T$ increase for increasing tank pressure.

The effect of initial ullage volume and ramp rates on the pressurant requirements for the pressurization period are as follows:

(1) Increased M_I/M_G for larger initial ullage volumes for a given ramp rate

(2) Increased M_I/M_G for increased ramp rates at a given initial ullage volume

Lewis Research Center,
National Aeronautics and Space Administration,
Cleveland, Ohio, May 27, 1969,
180-31-02-01-22.

APPENDIX A

VARIABLE GEOMETRY, HEAT LOSS TO TANK WALL, AND INTERNAL HARDWARE

The basic analysis used in this report for predicting pressurant gas requirements was developed by W. H. Roudebush in reference 1 for a cylindrical tank.

The major assumptions in the analysis of reference 1 are as follows:

(1) The ullage gas is nonviscous.

(2) The ullage gas velocity is parallel to the tank axis and does not vary radially or circumferentially.

(3) The tank pressure does not vary spatially.

(4) The ullage gas temperature does not vary radially or circumferentially.

(5) The tank wall temperature does not vary radially or circumferentially.

(6) There is no axial heat conduction in either the gas or the wall.

(7) There is no mass transfer (condensation or evaporation).

(8) There is no heat transfer from the pressurant gas to the liquid.

Experiments performed at Lewis (ref. 3) confirmed most of these assumptions. The experimental results indicated, however, that there is significant heat transfer from the gas to the liquid with resulting mass transfer.

For the purposes of this report, the analysis of reference 1 was modified for application to arbitrary symmetric tank shapes, and an attempt was made to incorporate the heat transfer from the gas to the liquid. The treatment of internal hardware (e.g., tank baffles, instrumentation) was also modified to correspond to the treatment of heat transfer to the tank wall.

The primary equations which deal with the pressurizing gas upon entering the tank are:

(1) The first law of thermodynamics

(2) The continuity equation

(3) The equation of heat transfer for a point in the tank wall

First Law of Thermodynamics

The form of the first law of thermodynamics used in the analysis in reference 1 for cylindrical tanks is

$$\frac{\partial T}{\partial t} = \frac{2h_c ZRT}{r\overline{M}PC_p}(T_w - T) - \overline{V}\frac{\partial T}{\partial x} + \frac{RTZ_1}{\overline{M}PC_p}\frac{\partial P}{\partial t} + \frac{RTZ\dot{q}_H C_H}{\pi r^2 \overline{M}PC_p}$$

Modifying this equation to account for both arbitrary symmetric tank shapes and internal tank heat sinks gives

$$\frac{\partial T}{\partial t} = \frac{2h_c ZRT}{r\overline{MPC}_p}(T_w - T)\left[1 + \left(\frac{dr}{dx}\right)^2\right]^{1/2} - \frac{\overline{V}\partial T}{\partial x} + \frac{RTZ_1}{\overline{MPC}_p}\frac{\partial P}{\partial t} + \frac{\dot{Q}_H}{C_p M_H} \tag{A1}$$

The first term on the right includes the effect of wall curvature. The last term, the energy lost to the internal hardware, is treated as the summarion of hardware components: (1) laminated thermoplastic, (2) stainless steel, and (3) copper. For the tanks in this investigation,

$$\frac{\dot{Q}_H}{M_H} = \sum_{\substack{\text{Hardware} \\ \text{components}}} \frac{A_H h_c (T_H - T_G)}{\rho_H V_H} \tag{A2}$$

Gluck and Kline, in reference 6, employed the free convection correlation to the pressurant gas (hydrogen, helium) for the pressurized transfer of liquid hydrogen:

$$\frac{h_c L}{k} = Nu = 0.13(GrPr)^{1/3} \tag{A3}$$

This correlation is used herein even though it was developed for cylindrical tanks. Pressurant gas transport properties were evaluated at the mean of the gas and wall temperatures.

Continuity Equation (Area = f(x))

The basic form of the continuity equation for a cylindrical tank is presented in reference 1 (eq. (24)) as

$$\frac{\partial \overline{V}}{\partial x} = \frac{Z_1}{ZT}\left(\frac{\partial T}{\partial t} + \frac{\overline{V}\partial T}{\partial x}\right) - \frac{Z_2}{ZP}\frac{\partial P}{\partial t}$$

The modified form of the continuity equation due to variations in tank radius with distance along the vertical axis becomes

$$\frac{\partial \overline{V}}{\partial x} = \frac{Z_1}{ZT}\left(\frac{\partial T}{\partial t} + \frac{\overline{V}\partial T}{\partial x}\right) - \frac{Z_2}{ZP}\frac{\partial P}{\partial t} - \frac{2\overline{V}}{r}\frac{\partial r}{\partial x} \tag{A4}$$

where Z_1 and Z_2 are defined in reference 1 as

$$Z_1 \equiv Z + T\left(\frac{\partial Z}{\partial T}\right)_P$$

$$Z_2 \equiv Z - P\left(\frac{\partial Z}{\partial P}\right)_T$$

The last term in equation (A4) evolves from the derivation as follows. For the one-dimensional expression for continuity,

$$\frac{\partial}{\partial x}(\rho \overline{V} A) + \frac{\partial}{\partial t}(\rho A) = 0$$

The substitution $A = \pi r^2$ is made where r is the position radius at location x along the vertical axis:

$$\frac{\partial}{\partial x}(\rho \overline{V} r^2) + \frac{\partial}{\partial t}(\rho r^2) = 0$$

The expression for density from the equation of state $\rho = \overline{M}P/ZRT$ is substituted:

$$P\frac{\partial}{\partial x}\left(\frac{\overline{V}r^2}{ZT}\right) + r^2\frac{\partial}{\partial t}\left(\frac{P}{ZT}\right) = 0$$

The following velocity equation is obtained after performing the partial differentiation and after rearranging terms:

$$\frac{\partial \overline{V}}{\partial x} = \left[\frac{1}{T} + \frac{1}{Z}\left(\frac{\partial Z}{\partial T}\right)_P\right]\left(\frac{\partial T}{\partial t} + \frac{\overline{V}\partial T}{\partial x}\right) + \left[\frac{1}{Z}\left(\frac{\partial Z}{\partial P}\right)_T - \frac{1}{P}\right]\frac{\partial P}{\partial t} - \frac{2\overline{V}}{r}\frac{\partial r}{\partial x}$$

When the expressions involving Z_1 and Z_2 are substituted in this equation, equation (A4) is obtained.

Tank Wall Heat Transfer

Reference 1 (eq. (18)) gives the heat-transfer equation which represents the change in wall temperature as a result of the convective process for a cylindrical tank:

$$\frac{\partial T_w}{\partial t} = \frac{h_c}{l_w \rho_w C_w}(T - T_w) + \frac{\dot{q}_w}{l_w \rho_w C_w} \tag{A5}$$

where $\dot{q}_w$ is the rate of heat addition per unit area to the tank wall from outside the tank.

For a small element of volume in the x-direction, equation (A5) can be written as

$$\rho_w C_w V \frac{\partial T_w}{\partial t} = h_c A(T - T_w) + \dot{Q}_w \tag{A6}$$

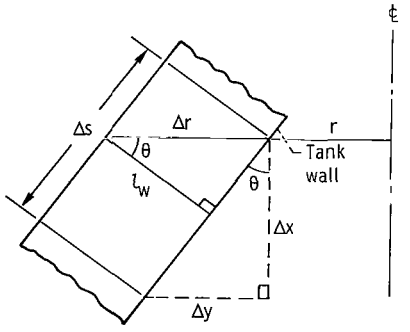

For a wall of arbitrary shape, the following is evident from the sketch:

$$\frac{A}{V} = \frac{2\pi r\,\Delta s}{2\pi r\,\Delta r\,\Delta x} = \frac{\Delta s}{\Delta r\,\Delta x} = \frac{1}{l_w}$$

Therefore, equation (A5) holds also for this case.

To account for the large mass concentration at the top of the tank, an equivalent l_w was used. This l_w was obtained by dividing the mass of the tank lid and flange connection by the surface area of the first net point.

APPENDIX B

EQUATIONS OF HEAT AND MASS TRANSFER AT THE GAS-LIQUID INTERFACE

The energy and continuity equations (A1) and (A4) should be modified to incorporate both heat transfer from the ullage gas to the liquid surface and mass transfer into the analysis.

The energy equation should incorporate two additional terms:

(1) The heat-transfer rate from the ullage gas to the liquid interface ($\dot{q}_{U \to S}$)

(2) The energy associated with mass transfer ($\dot{M}_t \lambda$)

Also, the boundary condition at the liquid surface should be revised to account for mass transfer. These additional terms can be related by performing an energy balance at the gas-liquid interface as done by W. A. Olsen in reference 7. The resulting relation, when the interface is saturated, is given by

$$\dot{q}_{U \to S} = \dot{q}_{S \to L} + \frac{\dot{M}_t}{A} \lambda$$

$$= \dot{q}_{S \to L} + \frac{\dot{M}_t}{A} (h_{VAPOR} - h_L) \tag{B1}$$

However, mass transfer was neglected since experimental data, presented in this report, indicate that the mass transfer rate $\dot{M}_t$ was relatively small for most cases (and hence, the energy associated with the mass transferred is small in comparison to $\dot{q}_{S \to L}$). The assumption was made that

$$\dot{q}_{U \to S} = \dot{q}_{S \to L} + \frac{\dot{M}_t}{A} (h_{VAPOR} - h_L) \cong \frac{d}{dt} (U_L) \tag{B2}$$

The term $d/dt(U_L)$ can be determined from experimental data. However, for the purpose of the analysis $\dot{q}_{U \to S}$ must be related to the ullage gas variables. This is done by the relation

$$\dot{q}_{U \to S} \equiv h_{c,L} (T_\delta - T_{sat}) \tag{B3}$$

The flow process is free convection flow of pressurant gas down the tank wall and then radially inward across the liquid surface.

The term T_{sat} was defined by the thermodynamic assumption of local equilibrium for a pure system with relatively small gradients as the saturation temperature corresponding to the tank pressure.

With regard to $h_{c,L}$, reference 8 developed an equation from boundary layer theory for forced flow across a horizontal, semi-infinite, constant temperature flat plate given by

$$Nu = \frac{h_{c,L}L}{k} = 0.664\left(\frac{\mu C_p}{k}\right)^{1/3}\left(\frac{L\overline{V}_L\rho}{\mu}\right)^{1/2} \tag{B4}$$

The velocity $\overline{V}_L$ of the gas across the liquid surface in terms of the gas velocity $\overline{V}_G$ down a vertical wall is given in reference 9 as

$$\overline{V}_L = 0.0975\,\overline{V}_G \tag{B5}$$

where $\overline{V}_G$, obtained by solving the integrated energy and momentum equations at the wall boundary, is given by

$$\overline{V}_G = 1.185\,\frac{\mu}{\rho Z}\,\frac{Gr^{1/2}}{\left[1 + 0.494\,(Pr)^{2/3}\right]^{1/2}} \tag{B6}$$

Combining equations (B5) and (B6) for $\overline{V}_L$ and substituting into (B4) give

$$Nu = \frac{h_{c,L}L}{k} = \frac{0.226\,(Pr)^{1/3}(Gr)^{1/4}}{\left[1 + 0.494\,(Pr)^{2/3}\right]^{1/4}} \tag{B7}$$

Equation (B7) shows that the conductance $h_{c,L}$ across the gas-liquid interface is similar in form to the empirical relation for free convection flow given in reference 10 as

$$Nu = \frac{h_{c,L}L}{k} = 0.14(GrPr)^n \tag{B8}$$

This equation with a value of $n = 1/3$, although somewhat arbitrary, is used in this investigation.

At this point, some choice of T_δ, which is consistent with the definition of $h_{c,L}$ and fits the data for $\dot{q}_{U \to S}$, (i.e., $d/dt(U_L)$) must be made.

In reference 11, which involved the pressurization of hydrogen with a low mixing diffuser and no liquid outflow, the adiabatic compression temperature given by $T_{ad} = T_o (P/P_o)^{(\gamma-1)/\gamma}$ was used as the choice for T_δ. This relation gave good agreement between analytical and experimental mass flux results.

However, for the conditions described in reference 11, appreciable condensation occurred. For greater ullage gas mixing (due to diffuser characteristics as well as the liquid outflow process), T_δ would be expected to be a higher value than T_{ad}. Reference 11 indicated that as T_δ increases there is a tendency toward evaporation - that is, away from the condensation results that occurred when the adiabatic temperature was used.

For the work described herein, T_δ was evaluated using the relation $\dot{q}_{U \to S} = h_{c,L}(T_\delta - T_{sat}) = d/dt\ (U_L)$ for a specific case. The value $d/dt\ (U_L)$ was determined from an experimental run where the expulsion time was approximately 452 seconds. For this condition T_δ was determined to be 1.18 times the adiabatic temperature, or approximately 41.7 K (75° R), for a tank pressure of 34.47×10^4 newtons per square meter (50 psia). This value of T_δ was used for all comparisons since most of the experimental ullage gas temperature profiles indicated a change in slope around 56 K (101° R).

Using equation (B8), as well as the values for T_δ and T_{sat} discussed above, gave the final form of the equation used to evaluate the heat transferred from the ullage gas to the liquid interface as follows:

$$\dot{q}_{U \to S} = \frac{k}{L}(0.14)(GrPr)^{1/3}(41.7\ K - T_{sat}) \tag{B9}$$

In order to incorporate liquid heating to the analysis, the term

$$-\frac{\dot{q}_{U \to S} A_L}{X_n V_\rho} \quad \text{or} \quad -\frac{k(0.14)(GrPr)^{1/3}(41.7\ K - T_{sat})A_L}{L X_n V_\rho} \tag{B10}$$

must be added to the right side of equation (A1).

APPENDIX C

RAMP ANALYSIS

An application of the work reported in reference 1 is the prediction of mass of pressurant for the ramp and hold period. A separate computer program which determines mass of pressurant as well as the tank wall energy requirements during the ramp and hold period is described herein. The same equations which deal with the expulsion period, as outlined in appendix A, are still applicable in the ramp and hold analysis to predict mass of pressurant and wall energy requirements. This analysis computes the gas temperatures in the ullage at any time during the pressure rise from the gas energy equation. The corresponding gas velocities are computed from the equation of continuity. The iterative method to be described shows how convergence is achieved in the solution of the gas energy and continuity equations.

The predicted mass of pressurant is based on an integration of the volume elements in the ullage at the end of the ramp and hold periods.

Because of the complexity of the equations involved in the iteration and because of the small amounts of pressurant required for the ramp when compared with the expulsion, no mass transfer or energy to the liquid is included in this analysis. Mass transfer requirements accounted for approximately 10 percent of the experimental pressurant requirements for the ramp period. Quantitatively, the entire mass of pressurant requirements for the ramp period was less than the expulsion period by a factor of 30 to 60 when the initial ullage was 5 percent of the tank volume.

INPUT DATA REQUIREMENTS

For the solution to proceed, a set of boundary and initial conditions are required. These conditions, which are the same for the expulsion as well as the pressurization, are as follows:

(1) At time $t = 0$, the values of gas temperature T and wall temperature T_w as functions of x, the position within the ullage

(2) On the boundary $x = 0$, the value of inlet gas temperature T as a function of time

(3) At the liquid surface, the value of gas temperature T, wall temperature T_w, and velocity $\overline{V}$ as functions of time (Although movement of the interface has been noted during the ramp pressurization period, no significant effect on the programmed output was noted with the value of $\overline{V} = 0$ at the interface.)

(4) Tank pressure P, outside heating rate $\dot{q}_W$, and inside hardware heating rate $\dot{q}_H$ as functions of time (Like the other initial conditions, the pressure P as a function of time or ramp pressure curve is defined by a discrete set of points which approximate a smooth curve. In regions or pronounced curvature, more points are needed for accurate definition than for linear portions.)

(5) Constant value of heat transfer coefficient h_c, or a correlating equation from which h_c may be evaluated at each net point from values of T, T_W, and P

(6) Tank radius as a function of axial distance down from the top of the tank

(7) Tank wall material properties: density ρ_W and specific heat $C_W(T_W)$

(8) Tank wall thickness (average membrane plus weld area thickness) as a function of axial distance down from the top of the tank

(9) Pressurizing gas properties: molecular weight $\bar{M}$, specific heat $C_p(T)$, and compressibility factor Z(P, T)

(10) Initial ullage height, total time of run, the number of net points in the initial ullage space

(11) The initial time step Δt used in following the pressure rise as well as establishing the points of computation

(12) If the hold period is to be included in the analysis, then the time for the end of the ramp must be specified

APPLICATION OF BASIC EQUATIONS

Reference 1 makes the substitution of $T_{w,i}$ from the finite difference form of (A6) into the finite difference form of the first law. Rearranging gives a quadratic in the gas temperature T'_i where the prime refers to a step forward in time and the quantities without the prime are evaluated at the previous time step:

$$T_i'^2 + \left[\alpha_i^*\left(1 + \bar{V}_i^* \frac{\Delta t}{\Delta x} - \omega_i^*\right) - T_{w,i} - \left(\frac{\dot{q}_w \Delta t}{l_w \rho_w C_w}\right)_i^*\right] T_i' - \alpha_i^*\left(\bar{V}_I^* \frac{\Delta t}{\Delta x} T'_{i-1} + T_i\right) = 0 \qquad \text{(C1)}$$

The quantity marked with the asterisk may be evaluated either at the beginning or the end of the time interval.

A difficulty can arise when evaluating the gas energy equation expressed by the previous quadratic. This occurs when the heat transfer takes place from the wall into the ullage gas. For this situation, the solution of the continuity equation provided negative gas velocities which made it impossible for equation (C1) to converge on the real roots.

At the start of the ramp (immediately after filling the tank), the initial wall temperature distribution in the ullage is higher than the gas temperature distribution. This is brought about since the wall surface above the liquid is exposed to the ambient temperature. But the ullage gas temperature near the liquid interface is close to the saturation temperature at one atmosphere.

The technique used when $T_{w,i} > T_i$ involved a direct substitution. The finite difference form of equation (A4) is

$$\overline{V}_i' = \frac{\left[T_i'\overline{V}_{i+1}' - \left(\frac{Z_1}{Z}\right)_i'\left(\frac{\Delta x}{\Delta t}\right)(T_i' - T_i) + \left(\frac{Z_2}{Z}\right)_i' \frac{T_i'}{P'} \frac{\Delta x}{\Delta t} (P' - P)\right]}{T_i' + \left(\frac{Z_1}{Z}\right)_i' (T_{i+1}' - T_i') - 2 \frac{\Delta x}{r_i} T_i' \left(\frac{\Delta r}{\Delta x}\right)} \tag{C2}$$

Substituting this value of $\overline{V}_i'$ for $\overline{V}_i^*$ in equation (C1) results in the following cubic equation:

$$b_i T_i'^3 + \left[\left(\frac{Z_1}{Z}\right)_i' T_{i+1}' + b_i c_i + \alpha_i^* \frac{\Delta t}{\Delta x} (\overline{V}_{i+1}' + d_i)\right] T_i'^2 + \left[c_i \left(\frac{Z_1}{Z}\right)_i' T_{i+1}'\right.$$

$$\left. + \alpha_i^* \frac{\Delta t}{\Delta x} \left(\frac{Z_1}{Z}\right)_i' \frac{\Delta x}{\Delta t} T_i - \alpha_i^* \frac{\Delta t}{\Delta x} T_{i-1}'(\overline{V}_{i+1}' + d_i) - \alpha_i^* T_i \frac{\Delta t}{\Delta x} b_i\right] T_i'$$

$$- \alpha_i^* \frac{\Delta t}{\Delta x} \left(\frac{Z_1}{Z}\right)_i' \frac{\Delta x}{\Delta t} T_i T_{i-1}' - \alpha_i^* T_i \left(\frac{Z_1}{Z}\right)_i' T_{i+1}' = 0 \tag{C3}$$

This cubic equation is solved for the gas temperature T_i'.

ANALYTICAL PROCEDURE

The analytical procedure uses a variable time increment Δt in following the pressure rise. With this technique, the iteration was stable over a range of inlet conditions and the results were consistent with the recorded data. The iteration proceeds in the following manner. A flow diagram is shown in figure 30 for reference.

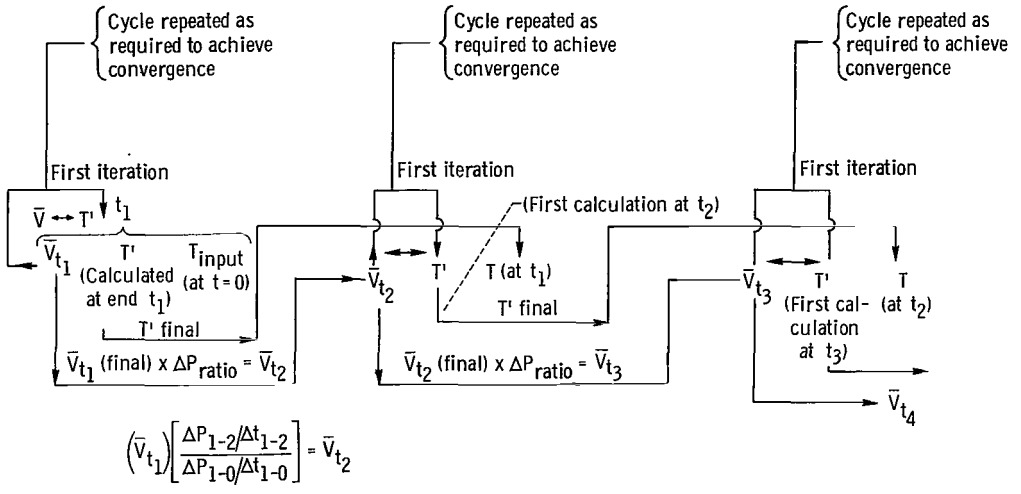

Figure 30. - Flow diagram showing temperature-velocity iteration in energy and continuity equations.

The initial velocity distribution is determined at time $t = 0$ by substituting the initial values of dT/dt from equation (A1) into equation (A4). For most of the ramp runs encountered in this investigation, an initial time increment of 1 second proved satisfactory.

TEMPERATURE CALCULATIONS FROM TOP TO INTERFACE

Since values of $\bar{V}$ have been obtained at each net point at time $t = T_1 = 0$, attention is turned to equation (C3) which is cubic in T'_i. During the iteration, the cubic equation (C3) is solved for the gas temperature T'_i starting at the point N_2 in figure 31. When this equation is first solved for the ullage temperature distribution, a value for T'_{i+1} is not available. A substituted value of T_{i+1} proved to be satisfactory as an initial guess to get convergence. All other quantities in equation (C3) are available from the initial conditions. The value for T'_{i-1}, the temperature at N_1, is known as a boundary condition.

The solution for T'_i at N_3 follows, and this procedure continues to calculate gas temperatures until the boundary at the interface is reached. The values for the corresponding wall temperatures are calculated using the finite difference form of equation (A6).

VELOCITY CALCULATIONS FROM INTERFACE TO TOP

Although the ullage temperatures are computed starting at the top (fig. 31), the

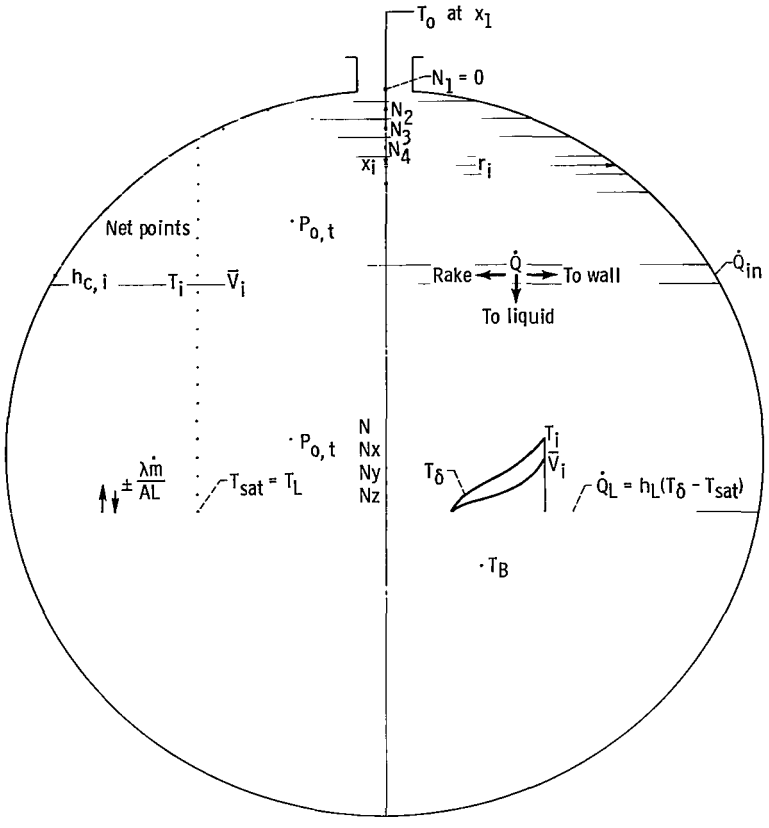

Figure 31. - Analytical model. (Coordinate system is positive in downward direction.)

velocity equation (C2) is used to calculate the ullage gas velocity starting with the point N_y near the interface. The velocity at the interface N_z, the boundary value, is zero with no expulsion.

The ullage gas velocity is calculated from point to point until the top of the tank is reached. The new velocities are used in equation (C3) along with previous values of T'_{i+1} and the temperature distribution is redetermined. This process is continued until convergence is achieved over the entire ullage. The time is then advanced to t_2 and a new set of velocities is determined.

COMPLETING THE SOLUTION

With the new velocities at time t_2, we evaluate equation (C3) again starting at point N_2 and terminating at the interface. A value for T'_{i+1} is always available from the previous iteration, although a substituted value of T_{i+1} is used as the first value.

The new values for T'_i at all the points for time t_2 are used to recompute the velocity distribution. This new set of velocities is then compared with the previous set

and convergence is assumed if the deviation is less than half of 1 percent for every velocity in the time set. A time step is then taken to t_3.

If convergence is not achieved after 40 iterations, the time step is reduced and the iteration process is reinitiated. Generally the reduction in time step becomes necessary only when there is a severe change in the slope of the ramp curve particularly in the early stages of the pressure rise.

For the new time t_3, the temperature T_i' in equation (C3) is determined from its converged value using the iterative method. This procedure continues to evaluate the gas temperatures and velocity distribution in the ullage for each time step taken in following the rate of pressure in the tank.

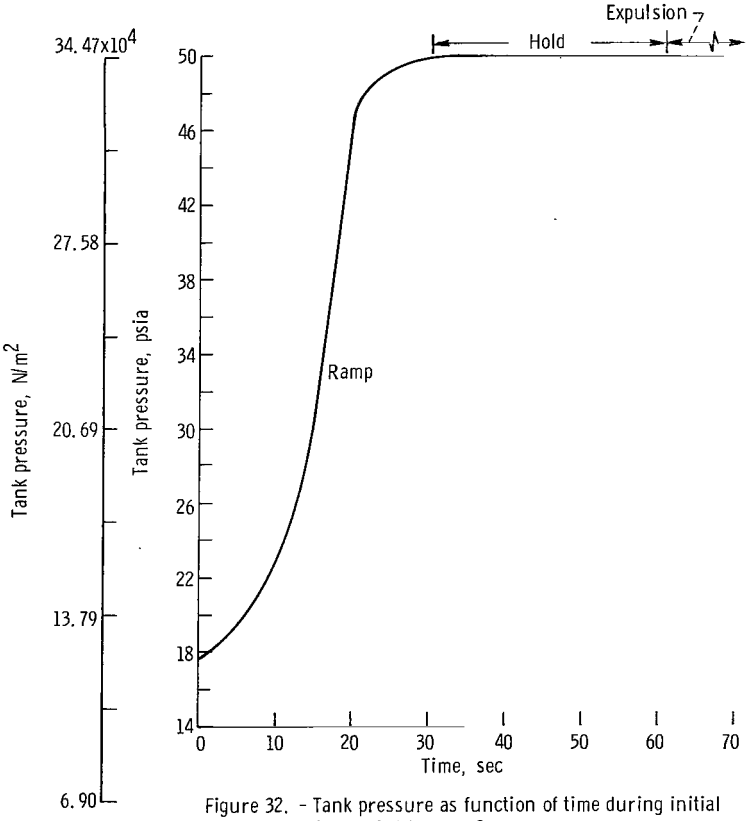

Figure 32. - Tank pressure as function of time during initial pressurization period for run 27.

The initial gas velocity distribution used in solving equation (C3) for each new time t is obtained from the previous time as follows:

$$V_{t,2} = V_{t,1} \frac{\left(\frac{\Delta P_{1-2}}{\Delta t_{1-2}}\right)}{\left(\frac{\Delta P_{0-1}}{\Delta t_{0-1}}\right)} \tag{C4}$$

This iterative procedure can be used for a constant pressure representing the hold period. However, for initiating the ramp, an actual pressure rise must be used. A typical example is shown in figure 32.

REFERENCES

1. Roudebush, William H.: An Analysis of the Problem of Tank Pressurization During Outflow. NASA TN D-2585, 1965.

2. Epstein, M.; Georgius, H. K.; and Anderson, R. E.: A Generalized Propellant Tank-Pressurization Analysis. International Advances in Cryogenic Engineering. Vol. 10, K. D. Timmerhaus, ed., Plenum Press, 1965, pp. 290-302.

3. DeWitt, Richard L.; Stochl, Robert J.; and Johnson, William R.: Experimental Evaluation of Pressurant Gas Injectors During the Pressurized Discharge of Liquid Hydrogen. NASA TN D-3458, 1966.

4. Stochl, Robert J.; Masters, Phillip A.; DeWitt, Richard L.; and Maloy, Joseph E.: Gaseous-Hydrogen Requirements for the Discharge of Liquid Hydrogen From a 1.52-Meter- (5-Ft-) Diameter Spherical Tank. NASA TN D-5336, 1969.

5. Stochl, Robert J.; and DeWitt, Richard L.: Temperature and Liquid-Level Sensor for Liquid-Hydrogen Pressurization and Expulsion Studies. NASA TN D-4339, 1968.

6. Gluck, D. F.; and Kline, J. F.: Gas Requirements in Pressurized Transfer of Liquid Hydrogen. Advances in Cryogenic Engineering. Vol. 7. K. D. Timmerhaus, ed., Plenum Press, 1962, pp. 219-233.

7. Olsen, William A.: Analytical and Experimental Study of Three Phase Heat Transfer with Simultaneous Condensating and Freezing on Cold Horizontal and Vertical Plates. Ph. D. Thesis, University of Connecticut, 1967.

8. Kays, W. M.: Convective Heat and Mass Transfer. McGraw-Hill Book Co., Inc., 1966.

9. Dickson, Philip F.: Large Gradient Mass Transfer. Ph. D. Thesis, University of Minnesota, 1962.

10. McAdams, William H.: Heat Transmission. Third ed., McGraw-Hill Book Co., Inc., 1954.

11. Olsen, William A.: Experimental and Analytical Investigation of Interfacial Heat and Mass Transfer in a Pressurized Tank Containing Liquid Hydrogen. NASA TN D-3219, 1966.

NASA-Langley, 1969 —— 28 E-5061

"The aeronautical and space activities of the United States shall be conducted so as to contribute . . . to the expansion of human knowledge of phenomena in the atmosphere and space. The Administration shall provide for the widest practicable and appropriate dissemination of information concerning its activities and the results thereof."

—NATIONAL AERONAUTICS AND SPACE ACT OF 1958

NASA SCIENTIFIC AND TECHNICAL PUBLICATIONS

TECHNICAL REPORTS: Scientific and technical information considered important, complete, and a lasting contribution to existing knowledge.

TECHNICAL NOTES: Information less broad in scope but nevertheless of importance as a contribution to existing knowledge.

TECHNICAL MEMORANDUMS: Information receiving limited distribution because of preliminary data, security classification, or other reasons.

CONTRACTOR REPORTS: Scientific and technical information generated under a NASA contract or grant and considered an important contribution to existing knowledge.

TECHNICAL TRANSLATIONS: Information published in a foreign language considered to merit NASA distribution in English.

SPECIAL PUBLICATIONS: Information derived from or of value to NASA activities. Publications include conference proceedings, monographs, data compilations, handbooks, sourcebooks, and special bibliographies.

TECHNOLOGY UTILIZATION PUBLICATIONS: Information on technology used by NASA that may be of particular interest in commercial and other non-aerospace applications. Publications include Tech Briefs, Technology Utilization Reports and Notes, and Technology Surveys.

Details on the availability of these publications may be obtained from:

SCIENTIFIC AND TECHNICAL INFORMATION DIVISION

NATIONAL AERONAUTICS AND SPACE ADMINISTRATION

Washington, D.C. 20546